UNIVERSITY OF TURKU

Material Selection for a Biodegradable Intravenous Implant

Master of Science in Technology Thesis
Materials Engineering in Health Technology
Department of Mechanical and Materials Engineering
Faculty of Technology

Author:
Nea Karppelin

1.4.2026
Turku

The originality of this thesis has been checked in accordance with the University of Turku quality assurance system using the Turnitin Originality Check service.

Master of Science in Technology Thesis
University of Turku

Subject: Materials Engineering (Materials in Health Technology)
Author: Nea Karppelin
Title: Material selection for a biodegradable intravenous implant
Supervisors: Professor Emilia Peltola, M.Sc. Valtteri Vinni, M.Sc. Iiro-Matti Mäkinen
Number of pages: 61 pages and 1 appendix
Date: 1.4.2026

The leading causes for incidence rates and mortality worldwide are rooted in cardiovascular diseases and their complications. The cardiovascular system is highly sensitive to any disruptions, and even a minor anomaly in the vascular tissue can lead to serious consequences. This has been a particularly important subject in medicine for a long time, and it continues to attract interest in research, which is no surprise. Implants can be used to achieve certain desired outcomes, by providing structural support for injured tissue. Usually, the human body tends to heal and attempts to restore the functionality of the injured tissue after some time. Considering that, biodegradable materials are currently of great interest, as they can support the tissue while degrading at the rate of the natural healing process of the body. As a result, the risk of long-term postoperative complications and infections can be reduced, as an implant material is removed through body's natural metabolic pathways once it is no longer needed.

Biodegradable polymers, specifically synthetic polyesters, have been studied and employed in many biodegradable implants for cardiovascular diseases. These polyesters include polylactide, PLA, polyglycolide, PGA, poly(lactide-co-glycolide), PLGA, and poly-ε-caprolactone, PCL. These polymers have an advantage of degrading and absorbing in the human body by producing nontoxic end products, carbon dioxide and water. Additionally, the degradation time and mechanical properties of these polymers can be tailored and tuned in a wide variety of ways.

In this work, biodegradable materials for an intravenous implant were investigated. Most importantly, the degradation time of the material is desired to be relatively rapid, during which the physical structure of the material is required to hold predetermined period of time. PLGA (50DL/50G) was examined in a laboratory experiment for its *in vitro* degradation. The effect of sterilization was included in the studies, as an implant must be sterile to ensure safe use. The sterilization methods used were hydrogen peroxide plasma and gamma irradiation. Sterilization was found to decrease the degradation time by approximately 20 %. This work demonstrated that the requirements for implants in terms of degradation time depend significantly on the intended use, and illustrated that it is more critical in this case to focus on the physical disintegration of the material during the degradation process than on the total degradation time. In that case, the intended use of the implant as structural support for tissue can be ensured for a sufficient period of time.

Key words: biodegradable implants, biodegradable polymers, biomaterials, PLGA, polyesters

Diplomityö
Turun yliopisto

Oppiaine: Materiaalitekniikka (Terveysteknologian materiaalien linja)
Tekijä: Nea Karppelin
Otsikko: ”Biohajoavan laskimonsisäisen implantin materiaalinvalinta”
Ohjaaja: Professori Emilia Peltola, DI Valtteri Vinni, DI Iiro-Matti Mäkinen
Sivumäärä: 61 sivua ja 1 liite
Päivämäärä: 1.4.2026

Sydän- ja verisuonitaudit sekä niistä aiheutuvat komplikaatiot johtavat sairastuvuus- ja kuolleisuustilastoja maailmanlaajuisesti. Verenkiertoelimistö on erityisen herkkä kaikenlaisille häiriöille, ja pienikin poikkeama verisuonikudoksessa voi johtaa vakaviin seurauksiin. Juuri siksi sydän- ja verisuonitaudit ovatkin olleet jo pitkään tärkeä tutkimuksen kohde lääketieteessä, eikä ole yllättävää että ne herättävät edelleen suurta kiinnostusta tutkimukselle. Implantin avulla vahingoittuneelle kudokselle voidaan tarjota rakenteellista tukea, minkä jälkeen kudos pyrkii yleensä parantumaan korjaten ja palauttaen toimintansa ennalleen. Biohajoavat implanttimateriaalit ovat tällä hetkellä suuressa suosiossa, sillä niiden avulla voidaan tarjota rakenteellista tukea parantuvalle kudokselle, ja samaan aikaan implanttimateriaali hajoaa kehossa sitä mukaan kun kudoksen luonnollinen paranemisprosessi etenee. Biohajoava materiaali poistuu kehosta luonnollisen aineenvaihdunnan mukana sen jälkeen, kun implantille ei ole enää tarvetta, minkä ansiosta operaatioiden jälkeisten pitkäaikaiskomplikaatioiden ja -infektioiden riskiä voidaan pienentää.

Biohajoavia polymeerejä, etenkin synteettisiä polyestereitä, on tutkittu ja hyödynnetty monissa biohajoavissa implanteissa, joilla hoidetaan sydän- ja verisuonisairauksia. Tällaisia polyestereitä ovat muun muassa polylaktidi (PLA), polyglykolidi (PGA), poly(laktidi-ko-glykolidi) (PLGA) sekä poly-ε-kaprolaktoni (PCL). Näiden polymeerien etuna on, että ne hajoavat ihmiskehossa täysin luonnollisiksi hajoamistuotteiksi, hiilidioksidiksi ja vedeksi. Lisäksi näiden polymeerien hajoamisaika ja mekaaniset ominaisuudet ovat laajalti muokattavissa.

Tässä työssä tutkittiin biohajoavia materiaaleja laskimonsisäistä implanttia varten. Tärkein vaatimus materiaalille oli suhteellisen lyhyt hajoamisaika, jonka aikana materiaalin rakenteellinen muoto oli pysyttävä riittävän pitkään. PLGA (50DL/50G) valittiin tutkittavaksi laboratoriotesteillä sen *in vitro* hajoamisen osalta. Steriloinnin vaikutukset otettiin huomioon tutkimuksissa, mikä on erityisen tärkeää, sillä implantti on steriloitava, jotta sen turvallinen käyttö voidaan varmistaa. Työssä tutkitut sterilointimenetelmät olivat vetyperoksidiplasmasterilointi ja gammasädetys. Steriloinnin havaittiin lyhentävän hajoamisaikaa noin 20 %. Tämä työ osoitti, että implanttien vaatimukset hajoamisajan osalta riippuvat merkittävästi käyttötarkoituksesta, ja havainnollisti, että kokonaishajoamisajan sijasta on tässä tapauksessa kriittisempää keskittyä hajoamisprosessin aikana tapahtuviin materiaalin rakenteellisiin muutoksiin. Tällöin kyseiselle implantille määritetty käyttötarkoitus kudoksen rakenteellisena tukena voidaan varmistaa riittäväksi aikaa.

Avainsanat: biohajoavat implantit, biohajoavat polymeerit, biomateriaalit, PLGA, polyesterit

Acknowledgements

I would like to express my gratitude to **Iiro-Matti Mäkinen** for making this work possible, and to **Miikka Frant** for guidance in the field of medicine. Additionally, thanks to my academic supervisors, **Emilia Peltola** and **Valtteri Vinni**.

For the help and support during the laboratory experiment, I would like to point special thanks to **Helmi Vuorinen**, **Kristofer Kolpakov**, **Tatu Hanski** and **Timo Laukkanen**. Your assistance was invaluable.

Lastly, thanks to **Omar Nasri** for your tips and tricks, assistance and support. And thanks to my friends and family.

The subject matter discussed in chapter 3.5.2 has been included in patent application FI20265304.

Abbreviations

EO	Ethylene oxide
FDA	Food and Drug Administration
HPU	Hyperbranched polyurethane
ISO	International Organization for Standardization
MDR	Medical Device Regulation
PBS	Phosphate-buffered saline
PCL	Poly-ε-caprolactone
PDLA	Poly-D-lactide
PDLLA	Poly-DL-lactide
PGA	Polyglycolide
PLA	Polylactide
PLAGC	Polylactide-co-poly(glycolide-co-caprolactone)
PLCL	Poly(L-lactide-co-caprolactone)
PLGA	Poly(lactide-co-glycolide)
PLLA	Poly-L-lactide
RCDs	Reduced carbon dots
SMP	Shape memory polymer
UV	Ultraviolet light

Table of Contents

1 Introduction

The vascular system is highly sensitive to disruptions [1], and any anomaly in the vascular tissue can lead to a vascular disorder or disease [2]. The leading causes for morbidity and mortality are in fact vascular diseases and their subsequent consequences [3]. Thus, it goes without saying why the vascular system is an extremely important field to study. Biomaterials are utilized in a wide range of different implants and medical devices for cardiovascular treatments in open surgeries and interventions, as well as in endovascular procedures [3]. However, these treatments still face drawbacks, such as immune rejection or limited durability [4]. The most outstanding limitation of conventional care methods is nonetheless their inability to promote a complete tissue regeneration and functionality restoration [4]. Those drawbacks have led to a rise of vascular tissue engineering interest [2]. Biodegradable polymers are particularly appealing in vascular engineering, including synthetic polymers like polyesters, that decompose into completely non-toxic substances in the human body [2]. Polyesters have been generally studied and employed extensively, for instance, vascular grafts with small diameters have been made of polyesters for decades now [2].

In this work, a biodegradable material for an intravenous implant is aimed to be determined. The material should be removed from the body within a predetermined period of time via hydrolytic degradation. Additionally, the material shall be safe for implantation into a human body and have certain mechanical properties. Furthermore, the material is desired to already have the Medical Device Regulation (MDR) approval by the European Union, and the Food and Drug Administration (FDA) approval by the U.S. Department of Health and Human Services.

Polyesters are the most used polymers in biodegradable stents [5], which resulted in a wider literature investigation of polylactide (PLA), polyglycolide (PGA), poly(lactide-co-glycolide) (PLGA) and poly-ε-caprolactone (PCL) in this thesis. PLA, PGA, PLGA and PCL are linear aliphatic polyesters that degrade via the hydrolysis of their ester bonds, and these polymers are mainly obtained by the ring-opening of the cyclic molecules [6, 7].

In addition to aliphatic polyesters, other approaches to the material selection are explored as well in this thesis. Apart from the plain use of aforementioned polymers, polymer blends are considered as well. Blending polymers allow broader modification possibilities and fine-tuning of material properties, which may be desirable or even required for the material to reach the

desired functionality. Furthermore, shape memory properties of polymers are also investigated and evaluated for the application of interest. More specifically, the interest in this case is shape memory effect that can be gained by mixing two polymers.

The effect of sterilization is critical to acknowledge, especially in the case of biodegradable polymers. These polymers are particularly susceptible to changes in polymer structure and morphology [8]. Often, the sterilization process causes undesired degradation [8], that significantly affects material properties [9], and thus the functionality of the implant. In this work, the suitability of different commonly used sterilization methods is evaluated.

1.1 Research Questions

The thesis addresses three research questions. These questions are the following:

1. What biodegradable materials are currently used in similar applications, and which of them seem most suitable for this case?
2. What material properties are the most critical in this context and how are these properties tested?
3. Is the tested material the most suitable option for the application in question?

The first question aims to map those materials already in use in similar applications and environments, and to evaluate the suitability of those materials for the application of interest. The second question aims to provide justifications for the material selection process through experimental laboratory work. The third question aims to result in final material selection, or to provide reasoning why the tested material is not the most appropriate and what should be considered in the future.

1.2 Thesis Content Summary

The following chapters focus on implantable biodegradable materials, their properties and degradation, and presenting experimental work and its results. Chapter 2 provides the definition of biocompatibility and a general description of biocompatibility of materials, as well as a description of the intended environment for the implant in this context, the venous system. In chapter 3, the most commonly used materials in similar applications, such as stents, are introduced. In addition, chapter 3 discusses the approaches and the issue of sterilization. Chapter 4 provides some general theory of the testing of biomaterials, which serves as

background for chapter 5, the experimental section. Chapter 6 presents the results of the laboratory work, and chapter 7 provides discussion of the material and proposes pinpoints for future work. Lastly, chapter 8 gathers the concluding marks.

1.3 Aim of the Work

The aim of this work is to examine biodegradable materials with appropriate properties in regard to the context, and evaluate their suitability for an intravenous implant. The work aims to result in a proper material selection, or to provide profound discussion of the tested material and propose changes. The material investigation is done through a comprehensive literature review on the currently used biodegradable materials in similar applications. One material is selected according to the evaluation of material properties reported in literature, and that material is tested for *in vitro* degradation. The effect of sterilization is also included in the work.

2 Background

The environment where the biodegradable intravenous implant is destined is the cardiovascular system, more specifically the vein, where the implant will be in direct contact with blood. The most important requirement for the material is that it shall be non-toxic and non-carcinogenic, and it should generate a body response only within reasonable limits. The material should not induce rejection or injury, and it must be considered safe. Thus, the focus here is on materials that already have MDR and FDA approvals. These approvals ensure that the material has been proven to be safe to implant into a human.

2.1 Implants

An implant is a device that is inserted into a human body intentionally, to either support or improve the functionality of a tissue or an organ. An implant is composed of one or more biomaterials, it may be inserted either partially or totally, and it can be either permanent or temporary. Biomaterial, or biomedical material, is defined as a material engineered in such manner that it can conduct any diagnostic or therapeutic intervention through interacting with components of a living organism, on its own or as a part of a complex system [10, 11]. Such manner may be an implant, for instance a vascular graft, or a medical device, such as a biosensor or an artificial heart, which are all designed to improve or restore the function of injured or decayed organs or tissues [11].

There is not a one perfect definition for biocompatibility that is used by every scholar in consensus [12]. In a consensus conference in Manchester, UK, in 1986, biocompatibility was agreed on the following definition: “the ability of a material to perform with an appropriate host response in a specific application” [10]. In 2008, Professor David Williams defined biocompatibility as: “the ability of a biomaterial to perform its desired function with respect to a medical therapy, without eliciting any undesirable local or systemic effects in the recipient or beneficiary of that therapy, but generating the most appropriate beneficial cellular or tissue response to that specific situation, and optimizing the clinically relevant performance of that therapy” [13]. In 2018, a consensus conference in Chengdu, China, was held to provide updated definitions of the terms in the field of biomaterials [10]. Based on that, the definition of biocompatibility was broadened to “the ability of a material to perform its desired functions with respect to a medical therapy, to induce an appropriate host response in a specific application and to interact with living systems without having any risk of injury, toxicity, or rejection by the immune system and undesirable or inappropriate local or systemic effects” [10].

Biocompatibility assessment does not have standard procedures, but rather relies on certain blood components in different conditions [12]. However, the International Organization for Standardization (ISO) has prepared general instructions and regulations for testing [10], and studies in animal models are used for biological testing [14]. Nevertheless, it is very important to acknowledge that the same biological response may not imply in human organisms, and even different human organisms may have varying responses depending on individual attributes [14]. Alongside the compatibility effects on the body that the implant possesses, it shall also be considered that the physiological environment affects the properties and behavior of the material [12]. Direct interaction with bodily fluids influences material's functioning parameters such as degradation, excretion and durability [12].

One of the key standard methods for biocompatibility evaluations and biomaterials examination is the ISO 10993 series for biological evaluation of medical devices, which comprises multiple parts [10]. Other important ISO standards for the intravenous implant include ISO 13485:2016 for quality management, ISO 14971:2019 for risk management, ISO 25539-1:2017 and ISO 25539-2:2020 for cardiovascular implants and ISO/TS 17137:2021 for absorbable cardiovascular implants.

2.2 Cardiovascular System and Biocompatibility

The role of the circulation, i.e., cardiovascular system, is versatile and crucial as it carries vital substances for organs and tissues, and transports metabolic waste from organs and tissues. It is responsible for carrying oxygen and nutrients to the cells [1], while also monitors human body temperature, controls blood pressure and volume, regulates hemostasis, and transports a wide range of other essential substances like hormones and inflammatory factors [3]. Heart, arteries that deliver blood to the tissues around the body, veins that carry blood back to the heart, and capillaries exchanging compounds between blood and tissue make up the circulation [3]. Vascular tissue must hold mechanical strength to support the dynamic blood and nutrient flow, while also maintain a suitable microenvironment biochemically [2]. The vascular system has a unique structure, and the walls of blood vessels are sensitive to any disruptions due to their complexity [1].

Vein walls are typically thinner than artery walls due to decreased blood pressure, but the diameter and the lumen of the veins are usually larger [3]. On estimate, veins contain about 60–75 % of all blood in the human body [15]. The walls of human blood vessels consist of three layers from the innermost: *tunica intima*, *tunica media* and *tunica adventitia*, which are all

composed of different structural components [3]. These structural components are the endothelium, muscular tissue, collagen and elastic elements [3]. Additionally, venous valves in veins ensure sufficient blood flow back to the heart by constant and cyclic opening and closing [15]. Figure 1 illustrates the wall structures of an artery and a vein.

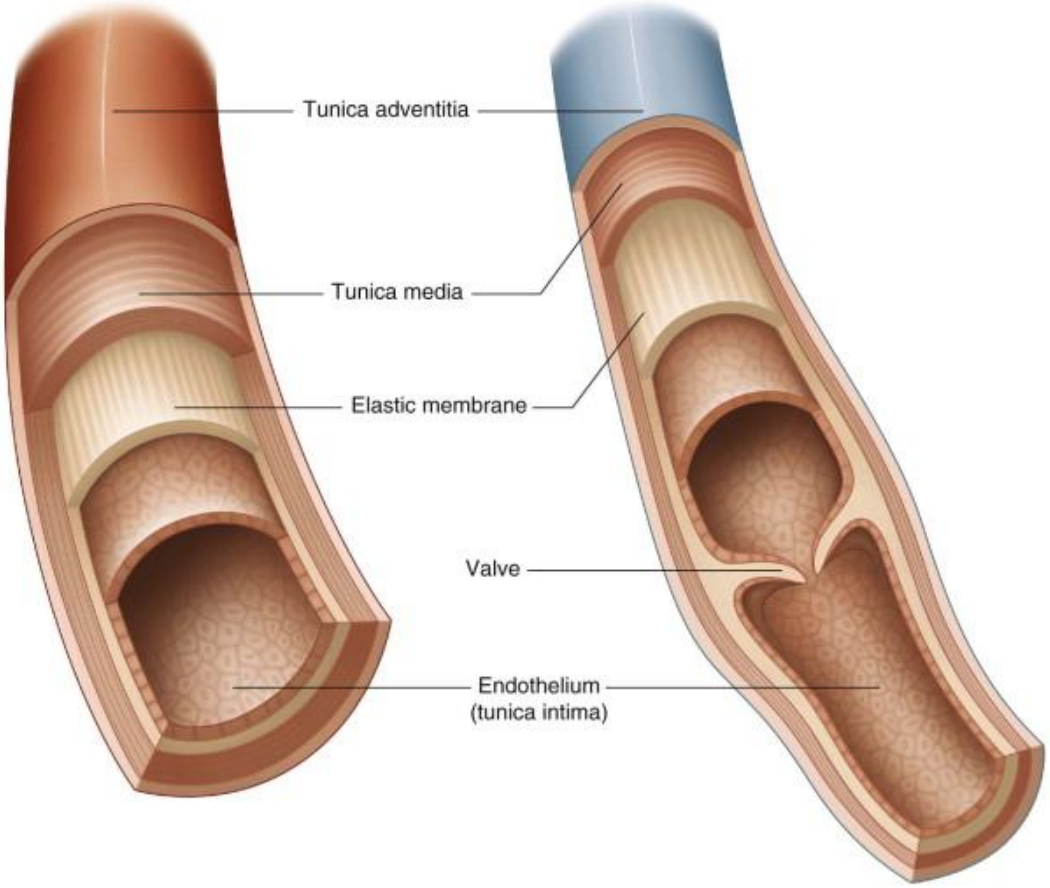

Figure 1. Vascular and venous wall structures. Copyright 2011, The Barral Institute. Published by Elsevier Ltd, reproduced with permission [16].

There are variety of treatment methods for vascular diseases involving medical devices and implants. These devices are precisely designed to specific vasculature environments, based on their different anatomic sites and functionalities [3]. Such devices include for example stents, vascular grafts and catheters [17]. Vascular devices come in direct contact with blood, and an introduction of an artificial material into a human body will always induce the natural defense process, which includes blood coagulation, inflammation and complement responses. If these processes are not considered and checked, the outcomes of the responses may result in serious consequences, such as stroke.

An implant is recognized as a foreign matter by human organism and immune system. Insertion of an implant is considered as an injury, which must be isolated and removed by the body. Injury of the tissue surrounding an implant is inevitable and will occur more or less, regardless of whether the implant is delivered surgically or minimally invasively. During implantation, a tissue injury is generated, which leads to an acute inflammation. The sequel of an acute inflammation is a chronic inflammation, that is followed by a formation of granulation tissue. Next, a foreign body reaction occurs, and lastly a formation of fibrous capsule, i.e., fibrosis. The attempt to isolate an implant by encapsulating it may lead to consequences such as device failure or malfunction.

In this context, a host response of the human body to an introduction of an implant and blood compatibility are critical factors affecting the performance and safety of the biomaterial. As many phases are happening at the same time during a host response, a natural response of blood to a foreign material starts with protein adsorption. Blood-plasma proteins coat the material's surface quickly, after which these proteins undergo conformational changes. These changes attract nonactivated platelets from blood stream to adhere onto the protein layer. The adhesion of nonactivated platelets induces platelet activation. After that, the platelets start to secrete activating factors, phospholipids and platelet factor 3's, which activate those platelets flowing nearby and induce the blood coagulation cascade. In addition, platelet activation causes an increase in fibrinogen-binding receptor expression, resulting in platelet aggregation and fibrin formation, as each fibrinogen protein is capable of binding with two platelets. This leads to formation of thrombus, followed by complement system and inflammatory response activations. A schematic representation of the blood response to foreign material is shown in Figure 2.

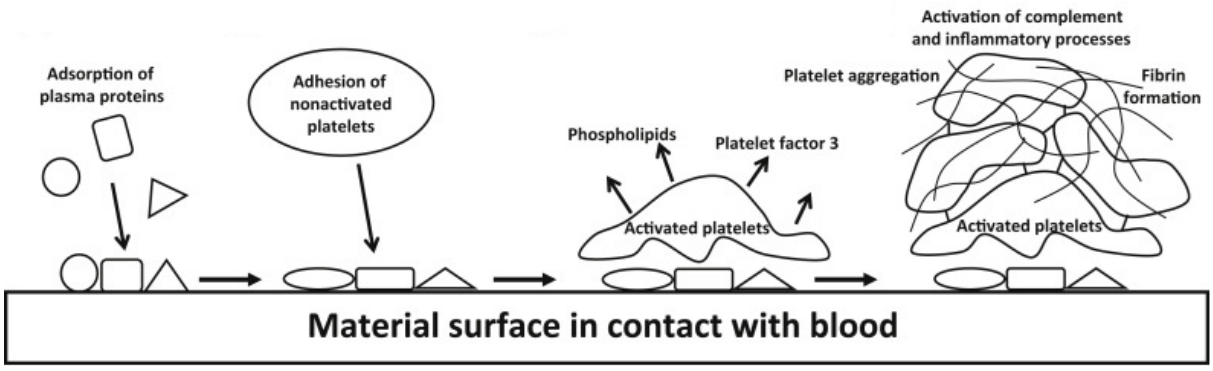

Figure 2. Blood-material contact upon implantation. Copyright 2020, Elsevier Inc., reproduced with permission [17].

3 Biodegradable Materials in Medicine

Material selection for implantable medical devices plays crucial part in device design and development. The material significantly affects the mechanical performance of the device [6], as well as the overall function and impact of the device. For the application of interest in this work, the material is required to be biodegradable, biocompatible and suitable for the intravenous environment. As a reference, vascular stents are utilized, since the properties of the implant in this context are required to be close to the properties of vascular stents. This chapter provides a comprehensive literature review on materials currently under investigation or already employed in applications that are similar to the interest. The chapter aims to result in the selection of a material or materials to be studied in the experimental section.

Initially, the materials used in intravascular medical devices or implants for treating, for example, coronary artery diseases, were mainly bare metals such as cobalt-chromium alloy or stainless steel [18]. Upon implantation these materials may, however, easily induce an inflammation and intimal hyperplasia [18], which is caused by the vascular operation that results in endothelial damage [19]. Intravascular restenosis is further a common sequel of intimal hyperplasia, having highly dangerous consequences [19]. Instead of permanent implantation of an implant into blood vessels, biodegradable implants may decrease the risk of restenosis or thrombosis [18].

A biodegradable implant can be composed of either metallic or polymeric material [5]. In the production of bioresorbable stents, major proportion of the used materials is composed of polymers [5], and especially polyesters are widely studied and employed polymers in vascular disease treatments [2]. Moreover, biologically corrodible metals like iron and magnesium have also been used [5]. Polymeric biodegradable materials have certain advantages over metallic materials, such as diverse structures and shapes that can be tailored to comply with the requirements of the desired intent [18], and they have tunable degradation time, and great biocompatibility as well as mechanical properties [2]. For the application of interest, these advantages are crucial.

Classification of biodegradable polymers includes natural and synthetic polymers [20]. Natural polymers are produced by a natural origin, such as microbial [20]. Polysaccharides are the most common and substantial group of natural biodegradable polymers [20]. Natural polymers include, for example, chitosan, collagen, albumin, cellulose and lignin [20]. The reproducibility

of multiple identical samples of natural polymers is low [21]. Natural polymers often lack strength and ability to resist physicochemical stimulus, which results in difficulties in keeping their properties and parameters constant [21]. Synthetic polymers, however, provide more precisely determined polymers, and their parameters and properties are more stable because the synthetic processing can be well controlled [22].

Various synthetic biodegradable polymer materials have been broadly examined and utilized in implants [18]. Most widely utilized group of polymers in bioresorbable stents is polyesters, according to their advantage of tunable biodegradability [5]. These materials include poly-L-lactide (PLLA), poly(lactide-co-glycolide) (PLGA), polyglycolide (PGA) and poly-ε-caprolactone (PCL) [5, 18, 23], which are all aliphatic polyesters. These aliphatic polyesters are an interesting group due to the versatility of their structural features [20]. A ring-opening polymerization mechanism may be used in synthesis of these polymers, which is a sustainable technique and allows scalability [20]. Scalability is an important feature in preparation, enabling the tuning of crystallization and hydrophilicity and those in turn affect the degradation properties [20].

Biocompatibility of polymer materials is influenced by the physicochemical properties of the polymers [12]. Cells and proteins interact with the polymeric material under certain conditions where parameters such as the surrounding temperature, pH and ionic strength are varying [12]. As an implant is introduced to blood, the first interactions occur with blood proteins [12]. Hydrophobic-hydrophilic character of polymers is one of the driving factors in protein adsorption onto the material upon implantation, and proteins are more prone to bind onto a hydrophobic surface [12]. The ratio between crystalline and amorphous structures has direct impacts on degradation properties of the material, induced immune reaction and cell responses including adhesion, proliferation and viability [12].

Biodegradable materials should resorb completely in the human organism without leaving any components of the material behind [12]. Biodegradable polymeric materials are hydrolyzed in the body, and the degradation products may be eliminated by leukocytes and giant cells [24]. This promotes the biocompatibility of these materials [24]. After the required time for the intended function, an implant erodes completely forming natural substances as reaction products [6], such as carbon dioxide and water [25]. Factors affecting the degradation rate of biodegradable polymeric implants are the polymer composition, molecular weight, morphology and glass transition temperature [24]. Amorphous regions degrade before the complete cleavage

of crystalline structures and cross-linkages [7]. A significant factor is the presence of free hydrophilic moieties in polymer chains [20]. Degradation properties may be tailored by modifying molecular weight, crystallinity and hydrophilicity or hydrophobicity of polymers [24].

A biodegradable polymeric implant can degrade through either surface or bulk erosion [22]. Surface erosion is directed solely on the surface of the degrading object, while bulk erosion takes place throughout the degrading object [22]. Surface degradation is greatly affected by the ratio of surface area-to-volume, and consequently by the shape and size of polymeric implant are defining input parameters [22]. On the other hand, bulk degradation is less affected by the size and shape, as the degradation occurs uniformly in the implant [22]. The defining parameters in bulk degradation are thus the overall amount of material and the material composition [22]. A schematic illustration of surface and bulk erosions is shown in Figure 3. Polyesters degrade through hydrolyzation of ester bonds, and thus the degradation time is also dependent on the availability of ester groups [22].

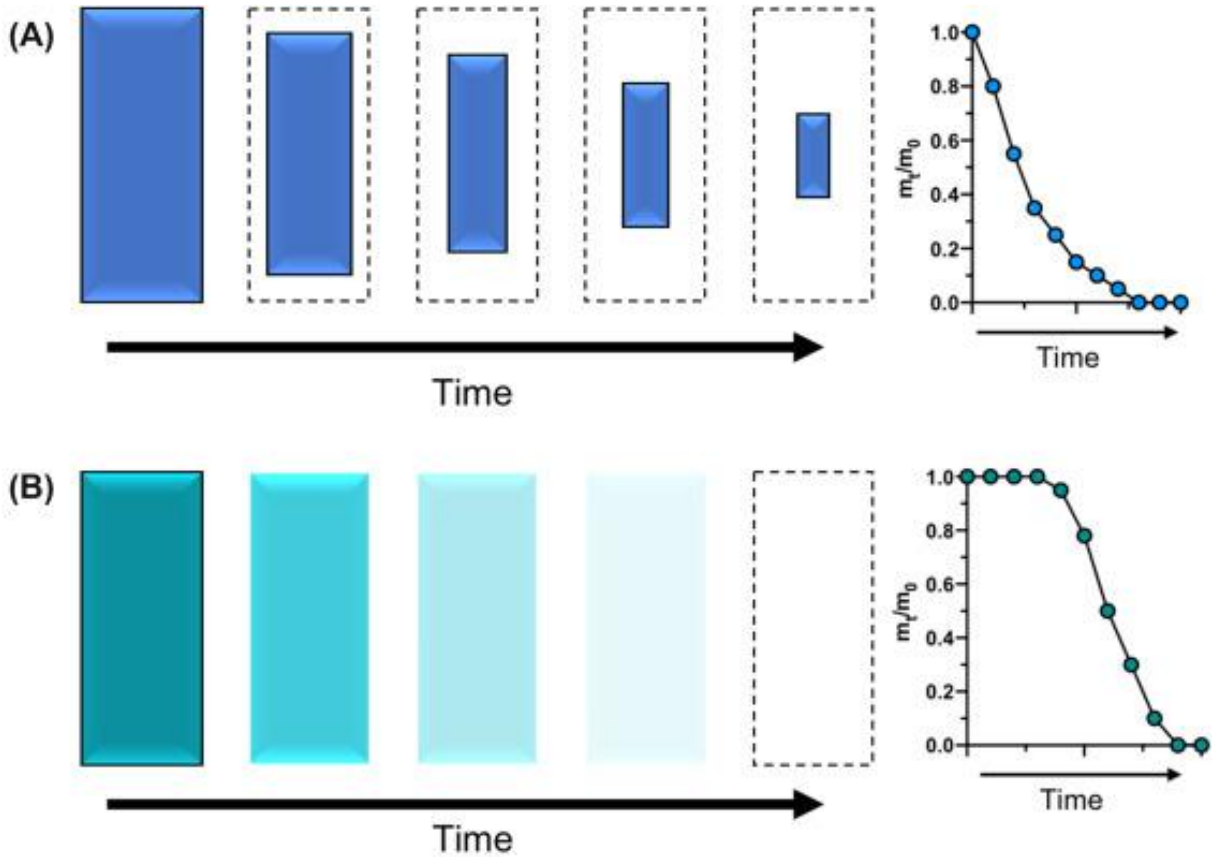

Figure 3. (A) Surface erosion and (B) bulk erosion by mass loss over time. Copyright 2020, Elsevier Inc., reproduced with permission [22].

Aliphatic polyesters exhibit bulk degradation [26]. In process of time, the bulk erosion is enhanced by the diffusion of water, which degrades the microstructure [27]. In addition, the degradation may also be catalyzed by an inflammatory reaction of the body, as an introduction of a polymeric object will induce a foreign body immune response [27]. The cells, such as macrophages, neutrophils and fibroblasts, secrete enzymes at the implant site in attempt to eliminate the foreign object, which exposes the object to biodegradation [27]. While the bulk of the polymeric object is degrading, a mass loss is not immediately experienced, but after a time of sufficient molecular weight loss in the bulk [14]. Only after the polymer chains have lost their molecular weight enough for the monomers to diffuse out, a mass loss is experienced [14].

The mechanical properties for the application of interest are required to be close to the mechanical properties of vascular stents. Thus, for reference, the requirements for a vascular stent may be examined. A vascular stent must comply with certain requirements regarding mechanical properties. These include yield strength of over 200 MPa, ultimate tensile strength of over 300 MPa and elongation to fracture of over 15–18 % [24]. However, it should be noted that the forces possessed by veins are significantly lower than what are experienced in arteries [1]. The pressures in veins and arteries vary greatly, which can be seen in Table 1, where the pressures of different sizes of arteries and veins are compared. As can be observed the table, the pressure in large arteries is 20 times higher than in corresponding veins, 10 times higher in medium-sized arteries, and about 6 times higher in small arteries.

Table 1. Comparison of pressures in arteries and veins [1].

Size	**Large**		**Medium**		**Small**	
Type of blood vessel	Artery	Vein	Artery	Vein	Artery	Vein
Pressure (mmHg)	100	5	100	10	90–95	15

In this case, the material is required to degrade at a rate that ensures the structural functionality of the implant for 4 weeks. The implant must stay in place for the total functioning time, without a risk of device migration in the vein. The device shall retain 50 % of the mechanical integrity, after 4 weeks of implantation. The application does not require radial strength, unlike stents do. The focus here are materials that already have MDR approval by the European Union and FDA approval by the U.S. Department of Health and Human Services. These approvals ensure that

the requirements of biocompatibility, nontoxicity, non-cytotoxicity and non-reactivity with other medical devices or substances, are fulfilled.

3.1 PLA

The most common polymeric material for biodegradable vascular stents is polylactide (PLA), also known as polylactic acid [25]. Other applications that have utilized PLA extensively are tissue scaffolds, sutures and vascular grafts [6]. PLA is biocompatible and nontoxic [6], and adverse reactions of the body towards PLA are rare with merely a few reports since the 1980's [27]. PLA is a polyester composed of lactide monomers [25]. Cyclic lactide monomer and the structure of PLA polymer are shown in Figure 4. General advantages of PLA include biodegradability, good mechanical properties, high biocompatibility and the ease of processing [25].

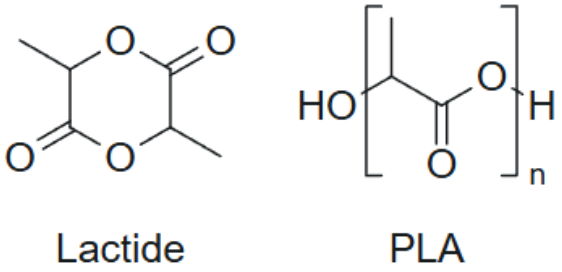

Figure 4. Chemical structures of cyclic lactide and PLA.

The polymerization mechanism used in synthesis of PLA can be polycondensation, ring-opening of a lactide molecule, or dehydration and condensation of the monomers of lactic acids [6]. Ring-opening polymerization offers reproducibility and batch to batch similarity of polymers [14]. It also allows the controlling of polymer chain construction and microstructure [14]. These advantages provide more precisely foreseeable polymer properties [14]. In ring-opening polymerization, the structure of a cyclic ester molecule is initiated to open with the use of an appropriate initiator or catalyst [14] to form a linear aliphatic polyester.

PLA is more prone to biodegradation in comparison to other polymers utilized in medical devices and implants, due to its water and oxygen semi-permeable characteristics [27]. The degradation mechanism of PLA is hydrolytic bulk erosion, during when the ester bonds of lactide polymer backbone are broken randomly [28]. PLA may be broken down into either monomers or oligomers of lactide, after which the free carboxylic acid moieties catalyze the reaction further [27]. The degradation pathway of PLA starts from hydrolysis of the polymer

chain, which produces lactic acid [14]. Lactic acid is further oxidized into pyruvic acid, which is processed into tricarboxylic acid in Krebs cycle [14]. Tricarboxylic acid is yet broken down into natural end products of carbon dioxide and water [14].

Lactic acid is a molecule experiencing chirality, meaning that it is optically active [6]. The two existing stereoisomers are D- and L-lactic acid [6]. These two enantiomers make up two different types of monomers, resulting in a total of three different forms of PLA [6]. The polymers are poly-L-lactide (PLLA), poly-D-lactide (PDLA) and poly-D,L-lactide (PDLLA) [6] The chemical structures of these polymers are shown in Figure 5.

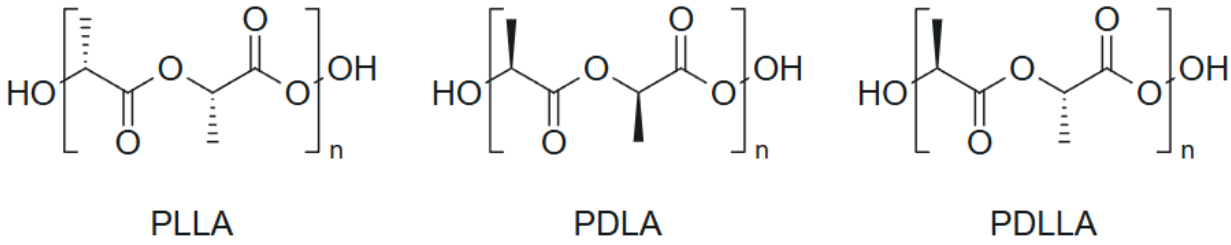

Figure 5. Chemical structures of PLLA, PDLA and PDLLA.

The different forms of PLA vary by their mechanical and degradability properties [27]. The orientation of molecular structure in different isomers causes variability in ester group accessibility to water molecules, which leads in different degradation times [22]. The degradation rate of PLLA is typically longer than the rates of PDLA and PDLLA [27], which is a consequence of a lower availability of hydrolysable ester bonds to water molecules. Structure of L-enantiomer is semi-crystalline, while D-enantiomer and the combination of L- and D-enantiomers are amorphous [27].

Naturally existing isomer is the L-lactic acid [28]. The crystallinity of PLLA is approximately 37 % [28]. Crystallinity is, however, affected by the processing factors and molecular weight [28]. Melting temperature is about 175 °C, while glass transition temperature is 60–65 °C [28]. Tensile strength of PLLA is 60–70 MPa, Young's modulus is 2–4 GPa, the elongation at break is 2–6 %, and the general degradation time is 18–36 months [29]. Degradation time of PLLA with high molecular weight has been studied *in vivo* with results from 2 to 5.6 years for complete degradation [28]. PLLA has been employed in various bioresorbable stents: ABSORB Bioresorbable Vascular Scaffold by Abbott Vascular, FORTITUDE/APTITUDE by Amaranth, MeRes by Meril Life Sciences, AnterioSorb by Arterius, DESolve by Elixir Medical, and MIRAGE by Manli Cardiology [5].

PDLA is hydrolyzed into D-lactic acid, which is first transformed into L-form by the liver after the hydrolyzation [14]. The structure of PDLA is amorphous, and the degradation rate is more rapid than the rate of PLLA [27], 12–16 months [29]. Tensile strength of PDLA is 40–55 MPa, Young's modulus is 1–3.5 GPa, and the elongation at break is 2–6 % [29]. PDLA has been used as a blend material with PLLA and L-lactic-co-ε-caprolactone, forming PLLA/PDLA/L-lactic-co-ε-caprolactone, in a bioresorbable stent ON-AVS BRS by OrbusNeich [29, 30].

PDLLA is a racemic combination of the two optically active enantiomers, D- and L-lactide [28]. Due to the racemic nature of the polymer where PDLA and PLLA are in random order, this blend polymer is amorphous [28]. Glass transition temperature of PDLLA is 55–60 °C [28]. PDLLA is more susceptible to biodegradation than PLLA [14], the degradation time being 3–4 months [5]. Tensile strength of PDLLA is 40 MPa, Young's modulus is 1–2 GPa, and the elongation at break is 1–2 % [5].

A low crystalline PDLLA has been used in a biodegradable stent ART BRS by Arterial remodeling Technologies [25]. ART BRS is composed of 98 % L-lactide and the remaining 2 % of D-lactide, and it degrades completely in 18–24 months [25]. It is notable that the proportion of D-lactide is much lower than L-lactide, which increases the degradation time significantly. PDLLA has also been used as a coating material in many bioresorbable stents, such as in ABSORB bioresorbable vascular scaffold by Abbott Vascular [29, 31], MeRes100 by Meril Life Science and XINSORB by Weite Biotechnology Co., Ltd. [25].

3.2 PGA

Polyglycolide (PGA), also referred to as polyglycolic acid, is polymerized from glycolide [6]. The chemical structures of glycolide molecule and its polymer PGA are illustrated in Figure 6. The polymerization mechanism for PGA is ring-opening of a cyclic glycolide molecule [6]. It is a biodegradable and hydrophilic polyester [2] that has a fast degradation rate with strength loss in 1–2 months [6].

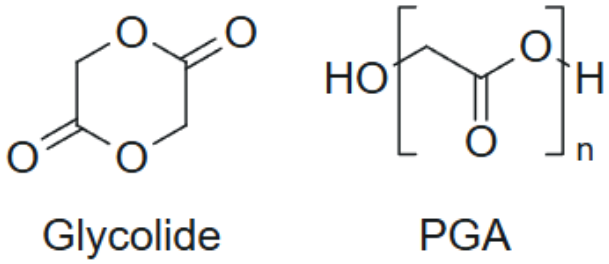

Figure 6. Chemical structures cyclic glycolide and PGA.

PGA's degradation pathway begins from the hydrolysis of polymer chains, that forms glycolic acid [14]. Glycolic acid may either be removed via urine elimination or processed into glycine [14]. Glycine may then be removed by urine elimination or processed further into serine, which is converted into pyruvic acid [14]. Pyruvic acid is broken down into tricarboxylic acid in Krebs Cycle, followed by transformation into carbon dioxide and water, like in the case of PLA [14].

PGA has a semi-crystalline structure [14], experiencing glass transition temperature of 35–40 °C and melting temperature of 225–230 °C [5]. PGA has one methyl group less than PLA, which makes it less hydrophobic and thus it degrades faster [5]. The degradation time of PGA is 4–6 months [29]. Tensile strength of PGA is 90–110 MPa, Young's modulus is 6–7 GPa and the elongation at break is 1–2 % [29].

PGA has been applied in a mixture material with PLA and poly-ε-caprolactone (PCL) (PLA/PCL/PGA) in a bioabsorbable stent XINSORB by Shandong Huaan Biotechnology Co., Ltd. [30, 32]. PGA has also been examined by Kwon et al. as material for a biliary stent and it was observed to experience rapid degradation of 8 weeks in *in vitro* evaluation [33].

3.3 PLGA

Poly(lactide-co-glycolide) (PLGA), also referred to as poly(lactic-co-glycolic acid), is a copolymer that has been approved for general and clinical research for cardiovascular diseases by the FDA and European Medicines Agency (EMA), and for clinical use by the FDA [34]. It is obtained by copolymerizing lactide and glycolide monomers [35]. The copolymerization is performed randomly [5], and it is achieved via either ring-opening method, which is the preferred method, or polycondensation method [7]. In the case of bioresorbable stents, copolymerized PLGA is produced to achieve longer degradation time of PGA by blending it with PLA [5]. Chemical structures of lactide, glycolide and their copolymer PLGA, where lactide monomer is on the left and glycolide monomer on the right, are shown in Figure 7.

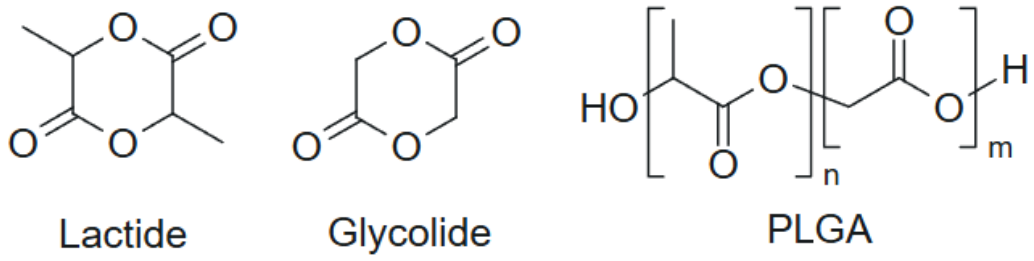

Figure 7. Structures of cyclic lactide, cyclic glycolide and PLGA.

The degradation of PLGA takes place via hydrolysis of the ester bonds, forming lactic acid and glycolic acid, that are further transformed via metabolic pathways into carbon dioxide and water in Krebs cycle [29]. PLGA is typically glassy and its structure depends on the lactide isomer [36]. PLGA with L-lactide has a crystalline structure, while PLGA with D,L-lactide has an amorphous structure [36]. Since the chains are quite stiff, PLGA has remarkable mechanical strength, which may be tuned by changing the copolymer ratio of lactide and glycolide [36].

Mixing PLA into PGA leads to the a more hydrophobic PLGA polymer and thus altering the hydrophobicity affects the degradation time [5]. PLA has an additional methyl group compared to PGA, therefore making it more hydrophobic than PGA [5]. The ratio of these copolymers determines the degradation rate [14]. In general, higher glycolide content results in faster degradation [7]. However, with a precise ratio of 50/50 content, the degradation time is the fastest and the addition of either monomer into PLGA50/50 increases the degradation time [7]. In *in vitro* and *in vivo* testing, PLGA50/50 possesses a degradation time of approximately 2 months [7]. The 50/50 composition is throughout amorphous, which decreases the degradation time significantly [14].

The degradation time of PLGA with a ratio of 85/15 of PLLA and PGA, respectively, is 12–18 months [29]. Tensile strength of PLGA (85L/15G) is 40–70 MPa, Young's modulus is 2–4 GPa and elongation at break is 2–6 % [29]. PLGA 85/15 experiences glass transition temperature of 45–50 °C [37].

The ratio of 50/50 of PDLLA and PGA possesses the degradation time of lower than 85L/15G [29]. The degradation time of PLGA (50DL/50G) is 1–2 months, and it has tensile strength of 40–50 MPa, Young's modulus of 2–4 GPa and the elongation at break of 1–4 % [29]. The structure of PLGA (50DL/50G) is amorphous and the glass transition temperature is 45 °C [5]. It is notable that this concerns only the racemic DL-blend of PLA.

PLGA has been applied as a bioresorbable scaffold material in FAST by Boston Scientific [38]. In addition, Biotronik has employed PLGA as a compound material with magnesium alloy, containing some rare earth metals in their DREAMS-1 bioresorbable scaffold [39], and Zorion Medical has employed PLGA with magnesium alloy in their FADES stent [40]. These scaffolds have been in either preclinical or clinical trials [38–40].

3.4 PCL

Poly-ε-caprolactone (PCL) is another biodegradable polyester [20], polymerized from ε-caprolactone by ring-opening mechanism [6]. FDA has yet approved a few medical devices composed of PCL, such as sutures and drug delivery systems [41]. PCL is broadly employed thermoplastic polymer as well, that experiences long degradation time of 2–4 years unmodified [2]. PCL is highly tough and elastic, but on the other hand it also exhibits high brittleness and poor thermal stability [2]. It has good processability and it can be easily combined with different polymers [2]. Chemical structures of caprolactone and PCL are shown in Figure 8.

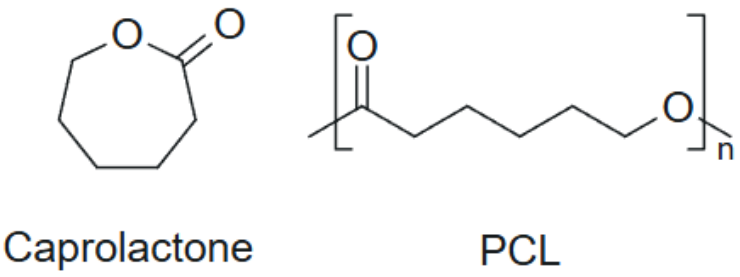

Figure 8. Structures of cyclic caprolactone and PCL.

The degradation process is mainly hydrolytic, as the ester bonds of PCL are broken down [6]. The lower frequency of hydrolysable ester bonds in PCL chains leads to a longer degradation rate compared to, for example, PLA's degradation time [41]. PCL is hydrolyzed into 6-hydroxycaproic acid, which has not been found to be either chronically or acutely toxic [14, 41]. Cells take the 6-hydroxycaproic acid in and transform it into acetyl CoA molecules via 2-β oxidation, after which the molecules enter the Krebs cycle [41]. The molecules are then metabolized and removed by kidneys without accumulating [41].

Like PLLA and PGA, PCL has a semi-crystalline structure [14]. However, the glass transition temperature is −60 °C, which is significantly lower than glass transition temperatures of PLLA and PGA [14]. This results in a lot more flexible structure of PCL [14]. The degradation time

of PCL is 24–36 months, and it has tensile strength of 25–35 MPa, Young's modulus of 0.2–0.4 GPa and the elongation at break of over 300 % [29].

Caprolactone has a hydrophobic nature, which increases the degradation time significantly [14]. To solve this, PCL has been copolymerized with more hydrophilic monomers like lactic acid and glycolic acid [14]. On the other hand, PCL has been copolymerized with PLLA and PGA, to achieve more flexible and softer compounds [14].

3.5 Other Approaches

3.5.1 Polymer Blends

The materials previously discussed have either already been utilized in biodegradable stents, such as PLLA in ABSORB bioresorbable vascular scaffold by Abbott Vascular, or those materials have been under extensive investigation. One of the main concerns for the application of interest is the degradation time. However, most of the previously discussed materials have relatively long degradation times. Because of that, blended polymer material may need to be used. Blending different polymers can decrease the total degradation time, as the orientation of variable monomers affects the packing of polymers. Other affecting factors are the altered ratio of functional groups, hydrophilicity, and a mixture of different glass transition temperatures and melting points. These factors may be utilized in the selection of material with appropriate degradation time. In terms of the degradation time, the most suitable materials seem to be PDLLA with a rate of 3–4 months and PLGA (DL50/G50) with a rate of 1–2 months.

An example of a polymer blend is PLA/PCL (70/30) [5]. PCL copolymerized with PLA in ratio of 70/30, respectively, has a much higher glass transition temperature than PCL as a homopolymer, being 20 °C [5]. Blending PLA with PCL decreases the degradation time of PCL to 12–24 months [5]. The structure of PLA70/PCL30 is semi-crystalline, and tensile strength is 2–4.5 MPa, Young's modulus is 0.02–0.04 GPa and elongation at break is over 100 % [5].

3.5.2 Shape Memory Polymers

Another thing to examine is whether the structural performance and the delivery of the implant can be assisted with a specific material selection. Shape memory characteristics of a material may be utilized to induce self-expanding or self-shrinking of the implant after it is delivered to its desired location. Shape memory polymers (SMP) are programmed to shift their shape once exposed to a specific stimulus [42], such as temperature, pH, light or solvent [43]. These

materials are forced into a temporary shape, which can be returned back to the fixed form after implantation [42]. Self-expanding allows the insertion of an implant via minimally invasive operation, as it is temporarily programmed into a small shape and upon implantation it recovers to the desired larger shape [42]. On the other hand, self-shrinking can be utilized to perform another types of functionalities, like self-tightening property of sutures [44].

There is a broad availability of polymers that express shape memory properties [42], and shape memory behavior based on solvent or thermal trigger may be observed to some extent in almost all kinds of polymers [43]. Shape memory effect is achieved by primarily two different types of crosslinkings, that the polymers form [42]. The crosslinks are either chemical or physical links that determine the permanent structure, called permanent crosslinks, and physical links that determine the temporary structure, called temporary physical crosslinks [42]. The temporary shape is gained by disintegrating the permanent crosslinks, which results in elastic energy storage [42]. The formed temporary physical crosslinks make up the temporary shape, which can be reversed back into the initial permanent shape with an external stimulus [42]. The shape recovery is induced by the stored elastic energy that is relaxed upon the physical temporary linkages are rearranged by the stimulus [42]. Biodegradable SMPs are mainly limited to being thermal, meaning that their shape recovery is induced by temperature changes [42].

An implant composed of polymeric material can be programmed to shift its shape based on human body temperature when implanted [45]. The material is processed by forcing it into the temporary shape in a temperature higher than the polymer's glass transition temperature (T_g) [45] or melting temperature (T_m) [42], which can both be considered a transition temperature (T_trans) that activates the shape shift [46]. Temperature is then decreased while keeping the shape in the deformed state, i.e., temporary shape [45]. Once the material is reheated above its T_trans, the polymer recovers back to its initial shape [47]. Figure 9 illustrates the shape shifting from a fixed shape to a programmed shape in relation to T_trans. SMP characteristics can be obtained directly in the production by molding or casting, or the product can be processed further after manufacturing to obtain the shape memory behavior [43].

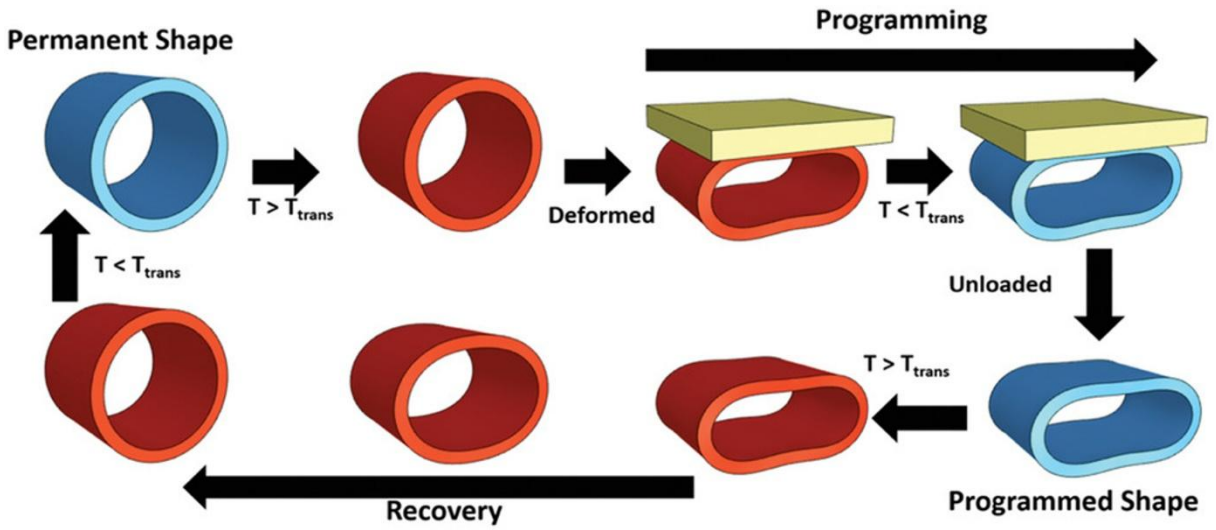

Figure 9. Schematic illustration of shape memory effect. Blue shape refers to temperature below transition temperature while red shape refers to temperature above transition temperature. Copyright 2020, John Wiley and Sons/Wiley-VCH, reproduced with permission [47].

In the case of SMPs for vascular stents, a desired Young's modulus is approximately 1–10 MPa [45], so that the stent is able to remain and function as intended [43]. By polymer processing, the value of Young's modulus is adjustable, since it is relative to the density of crosslinking [43]. SMPs are able to recover from strains as far as 400 % [45]. The shape shifting rate is dependent on the composition and the thickness of the stent [48].

In this context, self-shrinking properties are more interesting. Self-shrinking polymers responding to heat stimuli can be called thermo-shrinkable polymers [49]. Thermo-shrinkable polymers consist of two components, an amorphous and a crystalline segment that are crosslinked [49]. The amorphous region is responsible for elastic properties while the crystalline region is responsible for reversible transition [49]. In processing, the material is heated and elongated, after which it is cooled rapidly, resulting in crystallization of the crystalline polymers and stretching of the amorphous polymers [49]. This limits or restricts the mobility of the elastic segment's amorphous polymer chains [49], which locks-in the temporary shape. As the thermo-shrinkable material is heated again right above its melting point, the stretched amorphous chains are relaxed and the crystallite regions are melted, following a recovery of the initial shape [49]. The thermos-shrinking characteristics are dependent on crystallinity, crosslinking thickness and the orientation of amorphous polymer chains [49].

Relaxation of the stored elastic stress is the reason for self-shrinking [49]. Shape recovery is possible due to the crosslinked networks restricting the movement of the polymer chains, in a way that they are not able to slip over one another forming permanent deformation [49]. For

the polymer to stand great strain, the molar mass of the polymer must be high [49]. In addition, crosslinking enhances the storing of elastic energy [49]. The temperature at which the shrinking occurs is relative to the crosslinking degree, meaning that the more crosslinking, the lower the shrinking temperature [49]. As the heat-shrinking polymer consists of two different components, amorphous and crystalline, both components possess their own transition temperatures [49]. The component with higher T_{trans} determines the permanent shape, while the component with lower T_{trans} determines the temporary shape [49].

For the application of interest, a polymer material with T_{trans} close to human body temperature 37 °C is desirable, so that the shelf-shrinking is activated after implantation into the human body. To obtain self-shrinking behavior, the material is heated above T_{trans} of close to 37 °C and elongated into a larger temporary shape. Once the desired temporary form is gained, the material is rapidly cooled for the polymers to form temporary crosslinks. Upon implantation, the implant shrinks into its smaller initial shape by the trigger of human body temperature. The desired time for complete self-shrinkage is no more than 30 seconds, but at strict maximum of 60 seconds.

Duarah et al. have reported a study of a polymeric suture material with rapid self-tightening properties [50]. The material they created consisted of biodegradable hyperbranched polyurethane (HPU) and reduced carbon dots (RCDs), which were embedded into the HPU polymer matrix to enhance the mechanical and thermal properties [50]. Self-tightening occurred due to a shape memory property of biodegradable HPU/RCD composite, which was achieved at 37 °C ± 1 °C in 15 seconds when the sutures were stretched twice their length [50]. HPU/RCD with different ratios of RCDs showed shape recovery R_r>99.2–99.7 % ± 0.1–0.2 % and shape fixity R_f>99.1–99.6 % ± 0.2–0.3 % [50]. The shape recovery time was reported 15 s ± 1 s and self-tightening time 15–25 s ± 1 s [50]. The shape memory effect was improved with the incorporation of RCDs compared to pristine HPU [50]. This indicated an excellent shape memory effect of the HPU/RCD sutures. However, the degradation rate is relatively long as it was observed that at the time period of 90 days, the highest mass loss was only 7 % [50].

Choi and Park studied triblock PLGA/PCL/PLGA copolymers where the copolymer ratio of PLGA was 50/50 [51]. The degradation was observed to be 63 % of mass loss in 56 days while incubating at 37 °C in phosphate-buffered saline (PBS) medium [51]. The degradation time of PLGA/PCL/PLGA is close to the desired degradation time, thus making it a considerable material. For shape memory application, this blend could be programmed in a way that PCL

acts as the elastic region enabling the temporary shape, while PLGA acts as the permanent shape determining region. However, this polymer should be further investigated, since there are no reports of shape memory of that specific composition in literature.

In another study, Cha et al. reported a blended polymer, which was a blend of poly(L-lactide-co-caprolactone) (PLCL) with 50/50 ratio of L-lactic acid and caprolactone, and PLGA with 82/18 ratio of L-lactide and glycolide, respectively [52]. The degradation process and mechanical properties of PLCL may be controlled based on the ratio of monomers, which resulted in the use of that polymer instead of plain PCL that has a degradation time of over 24 months [52]. The shape memory behavior occurred in regard of T_g, and for the blend of PLCL50/PLGA50 the shape recovery was determined to take perfect place at 37 °C [52]. The R_f and R_r values for PLCL50/PLGA50 were both over 99 %, and the shape recovery of 100 % was reached within 15 seconds at 37 °C [52]. In addition, the authors stated that this polymer blend is a potential material for implants in blood-contact, based on their *in vitro* biocompatibility experiment [52].

Nardo et al. studied *in vitro* degradation of PLCL (poly(DL-lactide-co-caprolactone)/PLGA with composition of 25/75 and control samples of 100/0 and 0/100 [53]. PLGA consisted of 75/25 lactide and glycolide, while PLCL consisted of 86mol% DL-lactide [53]. PLCL25/PLGA75 showed weigh loss of 28.8 % ± 3.4 % at eight weeks of incubation in PBS, while the plain PLCL experienced weigh loss of 46 % and the plain PLGA weigh loss of 26.9 % ± 6.8 % at same point [53]. It can be observed that the degradation time of PLCL25/PLGA75 sets between the degradation times of the plain PLCL and the plain PLGA [53], which indicates that the ratio is a determining factor. It can be estimated that the addition of PLCL to the copolymer ratio likely decreases the degradation time, and by changing the ratio to PLCL50/PLGA50, the degradation time could reach the expected degradation time.

Table 2 concludes the desired material properties and the properties of presented materials and Table 3 the shape memory properties and degradation times of the presented materials for the shape memory application.

Table 2. The desired properties and the presented material properties. *No specific information available.

Material	Degradation time (months)	Tensile strength (MPa)	Young's modulus (GPa)	Elongation at break (%)	Structure	T_g (°C)	Ref.
PLLA	18–36	60–70	2–4	2–6	Semi-crystalline	60–65	[28, 29]
PDLA	12–16	40–55	1–3.5	2–6	Amorphous	*	[27, 29]
PDLLA	3–4	40	1–2	1–2	Amorphous	55–60	[5, 28]
PGA	4–6	90–110	6–7	1–2	Semi-crystalline	35–40	[5, 14, 29]
PLGA (85L/15G)	12–18	40–70	2–4	2–6	*	45–50	[29, 37]
PLGA (50DL/50G)	1–2	40–50	2–4	1–4	Amorphous	45	[5, 29]
PCL	24–36	25–35	0.2–0.4	>300	Semi-crystalline	–60	[14, 29]
PLA70/ PCL30	12–24	2–4.5	0.02–0.04	>100	Semi-crystalline	20	[5]

Table 3. Shape memory properties. *No specific information available.

Material	Degradation time (mass loss)	R_f (%)	R_r (%)	Shape recovery time (seconds)	T_{trans} (°C)	Ref.
HPU/RCD	7 % in 90 days	>99.1–99.6 ± 0.2–0.3	>99.2–99.7 ± 0.1–0.2	15 ± 1	37 ± 1	[50]
PLGA/PCL/PLGA	63 % in 56 days	*	*	*	*	[51]
PLCL50/PLGA50	*	>99	>99	15	37	[52]
PLCL25/PLCL75	28.8 % ± 3.4 % in 8 weeks	*	*	*	*	[53]

PLGA with a ratio of 50/50 of DL-lactide and glycolide has the most suitable degradation time and adequate mechanical properties. This material experiences the shortest degradation time of the presented polyesters, which is a consequence of the racemic blend of D- and L-lactides, and the amorphousness of the polymer. Thus, PLGA (50DL/50G) would be the selection of a material without shape memory.

To gain a shape memory property while having a decent degradation time, PLCL50/PLGA50 would be optimal. PLCL50/PLGA50 has shown great shape memory behavior in temperature

similar to human body temperature, which is optimal for the shape recovery to be activated upon implantation of the implant. Furthermore, it can be estimated that the material's degradation time is close to or slightly less than the degradation time of PLCL25/PLGA75. To decrease the degradation time even more, PLGA with a ratio of 50/50 DL-lactide and glycolide can be applied, as it has the most rapid degradation time. In addition, PLCL with DL-lactide could be applied, resulting in PLCL50(DL-lactide)/PLGA50(50DL/50G).

3.6 Sterilization of Biodegradable Polymers

Efficient sterilization of an implant is critical before insertion to achieve safe use by minimizing complications such as infection [9]. The aim of sterilization is to eradicate complication-causing pathogenic organisms [54]. Biodegradable polyesters are limited to only few sterilization methods due to their sensitivity to post-manufacturing processing [8]. Certain commonly used sterilization methods are destructive to these polymers' morphology and may cause undesired degradation [8], which may further modify the behavior and properties of the material [9]. Due to that, sterilization is important to include in the development of the implant at an early stage [54].

Dry heat sterilization is not a suitable method for PLA and PGA, since the use of high temperature above their melting or degradation temperatures may cause thermal changes in these polymers [54]. Heat combined with moisture, i.e., steam sterilization, which considerably increases the sterilization rate, can be generated with an autoclave [54]. However, steam sterilization possesses the same limitations as dry heat, regarding temperature and moisture sensitive polyesters [54]. A low temperature alternative is ethylene oxide (EO) gas, which does not generally cause polymer degradation [54]. EO is the most preferred sterilization method for polyesters like PLA and PLGA used in cardiovascular implants [54]. Sterilization with EO is based on its alkylating effect on the DNA of micro-organisms [55]. Still, EO has some drawbacks as well [55]. EO is a chemical sterilant, which may react covalently with polymers' functional groups, causing alteration of the structural and chemical configurations [55] and the mechanical properties [56]. The EO method is optimally performed at 55 °C [9], which is similar to or slightly higher than the glass transition temperatures of the presented polymers shown in Table 2. This could lead to structural alterations in the polymer, if the polymer's glass transition temperature is lower than at which EO sterilization is performed [9]. Furthermore, relative humidity on this method is typically required to be 35–80 %, which may result in hydrolytic polymer degradation during the sterilization process [9]. In addition, EO sterilization

may leave residues that are stated toxic and carcinogenic, and it can also restrain tissue regeneration [55].

Hydrogen peroxide (H_2O_2) is another chemical sterilant that can be applied as either vaporized or plasma [54, 55]. Hydrogen peroxide forms reactive oxygen species that cause oxidative stress to micro-organisms, resulting in their elimination [54, 55]. H_2O_2 sterilization is a suitable method for heat sensitive polymers, as it requires relatively low temperature [55]. Commonly, hydrogen peroxide gas plasma sterilization is performed at 40–65 °C, while vaporized form of hydrogen peroxide is done at 25–50 °C, and the sterilization process usually takes from 1 to 3 hours [55]. At the end of the H_2O_2 gas plasma sterilization process, H_2O_2 is converted into nontoxic products of oxygen and water [57, 58]. However, this method may cause alteration in chemical structures by the free hydroxyl radicals [55]. In addition, H_2O_2 has shown to cause degradation and changes in mechanical properties [55]. Compared to EO, H_2O_2 has more limitations in use due to the oxidative behavior, but it leaves no toxic residues and sterility can be achieved faster than with EO [54].

PLA and PLGA-based drug delivery systems in orthopedic implants are commonly sterilized with gamma radiation [54]. In gamma sterilization, gamma rays with high energy penetrate through the material, eliminating bacteria [54]. Being one of the most efficient sterilization methods, gamma irradiation also has its limitations when it comes to sterilizing polymeric materials [9]. Gamma irradiation may result in destructive effects in the polymer structure, such as crosslinking or chain cleavage, or oxidation [9], and biodegradable polymers are typically even more susceptible to bond cleavage by the high energy sterilization methods than nondegradable polymers [55]. These may affect the mechanical properties, for example strain or Young's modulus, change the glass transition temperature or promote degradation [9]. Additionally, although the gamma irradiation is typically performed at room temperature 20–22 °C [55], the temperature inside the gamma chamber may rise up to 40 °C during the irradiation process, as the temperature is not generally controlled [9]. Again, this temperature is close to the glass transition temperatures presented in Table 2.

Ultraviolet (UV) light sterilization is a method that utilizes specific wavelengths of UV light to eliminate microbes [54]. The method is cost-effective and simple, and it can be used to sterilize polymers due to its efficient antimicrobial properties [59]. UV sterilization is achieved at wavelengths of 210–328 nm, and the highest sterilization rates have been achieved at wavelengths of 240–280 nm [54]. However, poorer penetration ability compared to other

radiation based sterilization methods limits its applicability to only surfaces and water [54]. UV radiation may additionally cause harmful consequences to polymers, such as branching or polydispersity, or cause decrease in chain length or molecular weight [59].

The previously discussed sterilization methods and their suitability for biodegradable polymers are summarized in Table 4.

Table 4. Advantages and limitations of sterilization methods.

Sterilization method	Advantages	Limitations	Suitability	Ref.
Dry heat	High temperature No moisture	Temperatures used are above the melting points or degradation temperatures	Not suitable	[54]
Autoclave	Increased sterilization rate compared to dry heat	Moisture	Not suitable	[54]
EO	Low temperature Does not generally cause degradation	May react with polymers May leave toxic and carcinogenic residues or restrain tissue regeneration	May be suitable	[55, 56]
H_2O_2 plasma	Low temperature Leaves no toxic residues Sterilization faster than with EO	May alter chemical structure May cause degradation and changes in mechanical properties Does not have as efficient penetration ability as EO	May be suitable	[54, 55]
Gamma irradiation	Low temperature Does not leave any residues	May result in destructive effects in polymer structure, e.g., bond cleavage	May be suitable	[9, 54, 55]
UV	Simple and cost-effective	Poor penetration Limited to only surfaces and water May cause decrease in polymer chain length or molecular weight, polymer branching, etc.	May be suitable	[54, 59]

4 Testing of Biomedical Materials

In the experimental section, the material of choice is tested for its applicability to the intended use, in terms of *in vitro* degradation time. This chapter provides background information and theory for that experiment and also a theory of testing the mechanical properties of biomaterials. Examination of *in vitro* degradation allows the evaluation of *in vitro* degradability by giving an insight into the degradation behavior and profile of the polymer [26].

Degradability and the degradation profile are of critical interest and strictly defined parameters of the implant's performance in this context. The previously discussed aliphatic polyesters have mainly a characteristic of hydrolytic bulk degradation. Degradability testing should be done in a well-organized manner, and the methods used should be well defined and controlled [26]. PBS of 7.4 ± 0.2 pH is a common solution used for degradability testing, along with temperature of 37 °C ± 1 °C [26]. These conditions replicate the physiological environment of the human body to some extent, but it is notable that it does not mimic the human organism perfectly, as it does not involve, for example, any inflammatory factors or physical forces [26].

ASTM F1635 is a standard method for *in vitro* hydrolytic degradation testing of polymeric surgical implants, that includes guidelines for testing [26]. Lindsay et al. gathered the main points of ASTM F1635; the mass ratio must be larger than 30:1 between solution and the sample, there must be three or more samples per one testing point, the soaking dish must be sealable, the samples must be sterilized and packed corresponding to the product, and the samples must be removed from the experiment after drying and weighing [26]. Moreover, ISO 13781:2017 contains standard guidelines for *in vitro* degradation studies of implants composed of poly(lactide) and/or its blends and copolymers. ISO 13781:2017 states that the pH must be monitored at each testing point or at least every 6 weeks from a minimum of two soaking baths [60].

Ekinci et al. studied the hydrolytic *in vitro* degradation behavior of PLA films according to ISO 13781:2017 [61]. They used PBS solution with pH of 7.4, that was kept constant at 7.4 ± 0.2 [61]. The samples were immersed in 30:1 or greater ratio of PBS solution, measured by mL per grams [61]. pH was monitored at every 14 days point and changed if pH was not in the target range [61]. Degradation was determined by water absorption and mass change [61]. Water absorption refers to the amount of water that the material has taken in from PBS solution, and mass change is a result from degradation and out-diffusion of oligomers and monomers [61].

Water absorption was defined by weighing samples that were undried but wiped to remove any excess solution [61]. Water absorption percentage was then calculated following equation 1:

$$\mathrm{WI}(\%) = \frac{\mathrm{m_{undried}} - \mathrm{m_0}}{\mathrm{m_0}} * 100\ \% \quad (1)$$

where $\mathrm{WI}(\%)$ is the water absorption by percentage, $\mathrm{m_0}$ is the native weight of the sample and $\mathrm{m_{undried}}$ is the weight of the undried sample [61]. To determine mass change, vacuum oven was used to dry the samples from any PBS solution [61]. Drying conditions in the vacuum oven included 51 cmHg and 30 °C, and the films were dried for 48 hours [61]. Mass change was calculated according to equation 2:

$$\mathrm{MC}(\%) = \frac{\mathrm{m_{dried}} - \mathrm{m_0}}{\mathrm{m_0}} * 100\ \% \quad (2)$$

in which $\mathrm{MC}(\%)$ is the mass change by %, $\mathrm{m_0}$ is the native weight of the sample and $\mathrm{m_{dried}}$ is the weight of the dried sample [61].

In a research conducted by Min et al., *in vitro* degradation of a biodegradable multiblock polymer polylactide-co-poly(glycolide-co-caprolactone) (PLAGC) was examined [62]. Polymer samples that were 0.1 mm thick were bathed in 0.1 M PBS where pH was 7.4, while temperature was kept at 37 °C by a thermostat [62]. A fresh PBS solution was changed after every week [62]. Distilled water was used to gently clean the samples, followed by drying in vacuum conditions at normal room temperature, after which weighed before and after the experiment in order to determine weight loss during the experiment [62].

Nardo et al. performed *in vitro* degradation testing on PLCL/PLGA films of 10 mm x 30 mm in size [53]. The samples were soaked in PBS of 7.4 pH, and they were incubated at 37 °C [53]. 6 mL of PBS was used for one sample, and a fresh solution was changed every 2 weeks [53]. At weeks 1, 2, 4, 6 and 8 the samples were taken out from the degradation solution and dried at room temperature in vented space for a week after which they were weighed [53].

Another study conducted by Duarah et al. reported *in vitro* degradation examination of HPU/RCD material [50]. Film samples of 0.5 mm ± 0.01 mm thick were immersed in 0.1 M PBS solution in a shaking incubator at 37 °C [50]. Shaking incubator was in movement of 30 rpm, and the experiment was carried out for 90 days [50]. The samples were weighed, and the mass loss was determined at 30-, 60- and 90-days points [50]. Rinsing under deionized water and drying at 37 °C preceded weighing of the samples [50]. PBS solution was measured by the

weight in 3:1 relation to the sample weight [50]. Degradation was determined via weight loss, following equation 3 [50]:

$$\text{Degradation}(\%) = \frac{W_0 - W_1}{W_0} * 100\ \% \quad (3)$$

in which W_0 is the original dry weight and W_1 is the weight of a dry sample after degradation [50]. As can be observed, equations 2 and 3 are quite similar.

Schliecker et al. also investigated the hydrolytic degradation of a polymer by determining water absorption and mass loss [63]. The polymer under their investigation was poly(lactide-co-glycolide), that was prepared into films [63]. Schliecker et al. used the same kind of equation as equations 2 and 3 for calculating mass loss, but the water absorption was defined by equation 4 [63]:

$$\text{Water absorption}(\%) = \frac{W_w - W_d}{W_d} * 100\ \% \quad (4)$$

where W_w is the weight of a wet sample and W_d is the weight of a dry sample after degradation [63]. As can be seen, equation 4 uses wet and dry weights of the degraded sample, while equation 1 defines the water absorption by the native weight of undegraded sample and the wet weight of degraded sample.

All types of biomaterials, including ceramics, metals and polymers, have different mechanical responses and properties. Polymeric materials differ significantly from metals and ceramics in terms of deformation and stress-strain behavior [64]. Thermoplastic polymers, including aliphatic polyesters like PLA, PLGA and PCL, are broadly used in medical applications [65]. Thermoplastics are referred to being pseudo-ductile, meaning that as the usual cause of ductile deformation is found in dislocations, those are not found in these polymers [64]. The deformation of these polymers is driven by crystallization and necking [64]. Under tensile stress the polymer chains begin to align organized at a specific point of the object, leading to local crystallization, which is followed by necking [64]. After necking is initiated, the deformation proceeds consistently, and when stress is applied steadily, the deformation keeps continuing as a function of time [64]. As a result of the necking, the area of deformation grows large [64]. Lastly, the ultimate failure of the polymer is achieved by the formation of microvoids, which ultimately merge together, creating the fracture [64].

Tensile strength, compression strength and flexural properties are some of the key mechanical properties of the implant material in this case, due to the forces possessed by the intended intravenous environment. Hyuk Im et al. performed tensile and compression experiments on biodegradable vascular stents [66]. Testing for tensile strength was performed by using a tensile extension machine at a speed of 10 mm per minute [66]. The testing was based on ASTM D2256 standard [66]. Compression testing was performed on spiral samples, based on ISO 25539-2 standard for vascular stents [66]. The compression was applied at a speed of 10 mm per minute [66]. The samples were compressed 60 % radially, after which tension was released and the recovery of the samples was calculated by equation 5 [66]:

$$\text{Recovery rate}(\%) = \frac{\mathrm{D}_{\mathrm{compressed}}}{\mathrm{D}_{\mathrm{original}}} * 100\ \% \tag{5}$$

where $\mathrm{D}_{\mathrm{original}}$ is the original diameter of a sample and $\mathrm{D}_{\mathrm{compressed}}$ is the diameter of a compressed sample after tension release [66].

Lin et al. studied the mechanical properties of vascular stents that were made of biodegradable polyvinyl alcohol yarns [67]. They studied the compression strength and bending property of stent samples [67]. In the compression testing, the compression was applied at a speed of 1 mm per minute, while the displacement was set to 2 mm [67]. The bending property testing was conducted by bending the samples from both sides simultaneously up until 2 cm distance [67]. The bending was defined by diameter change of the stent samples, which was measured from the bending point before and after the test [67]. Following equation 6, the diameter variation was calculated [67]:

$$\text{Diameter Variation Rate} = \frac{\text{Diameter of a lengthwise} - \text{Bent sample}}{\text{Initial diameter of a sample}} * 100\ \% \tag{6}$$

The bending property was investigated because of the complicated nature of blood vessels [67]. The cardiovascular system consists of a variety of twists and it is highly branched, which shall be noted when delivering an implant into the vessels by minimally invasive methods [67]. When the implant is delivered into a blood vessel, it must withstand the bending forces possessed by those complicated vessels [67].

5 Experimental

In this chapter, hydrolytic *in vitro* degradation process of poly(lactide-co-glycolide) (50DL/50G) is studied. PLGA (50DL/50G) is chosen for experimental studies due to its approvable rapid degradation time and adequate mechanical properties. The primary focus here is the effect of sterilization on the degradation profile, and the total time of visibly observed complete degradation, that indicates how long the material is capable of holding its structure and thus its function.

The polymer should hold its structural shape for up to 4 weeks. Given that PLGA should experience bulk degradation, the polymer should keep its shape for quite some time before a clear degradation is visibly observed, after which a sudden burst of degradation should occur (see Figure 3). The degradation is studied through imaging and analyzing the documented samples, and by determining water absorption and weight loss. When no traces of the polymer are visibly observed, the experiment can be considered complete. This is because, in this case, the most important thing is to define how long the material will be able to fulfill its function by holding its shape.

In the following experiment, two different sterilization methods were chosen to examine and compare the effects of those methods. The methods chosen were hydrogen peroxide plasma treatment and gamma irradiation. Additionally, a control group of unsterilized samples was investigated. Samples are later referred to as plasma-PLGA, gamma-PLGA and control-PLGA, respectively. Degradation studies were carried out with unsterilized samples and gamma-sterilized samples. These samples were imaged at predetermined intervals, through which the degradation is analyzed. Furthermore, the precise degradation of the gamma-sterilized samples was determined by weighing water absorption and mass loss during the studies at predetermined points.

5.1 Sample Preparation

Samples for degradation studies were fabricated by first preparing thin polymer sheets that were cut into slices. PLGA (50DL/50G) pellets (Resomer® RG 503 H, Poly(D,L-lactide-*co*-glycolide), acid terminated, M_w=24,000–38,000, purchased from Merck) were placed onto a metal plate that was covered by a non-stick aluminum foil (Reynolds Wrap® Non-Stick Aluminum). The polymer was heated on the metal plate on a hot plate that was set to 236 °C for 10 minutes. Once the pellets got softer, they were positioned with a metal spatula in a way

that no large empty spots were left in between as the pellets melted together. Another metal plate covered by non-stick aluminum foil was set on top of the soft melted pellets. An 800 mL beaker filled with water was placed on top of the top metal plate to apply additional weight, which made the polymer sheets thinner. The polymer was heated in between the metal plates for 5 minutes. The melting set-up is shown in Figure 10.

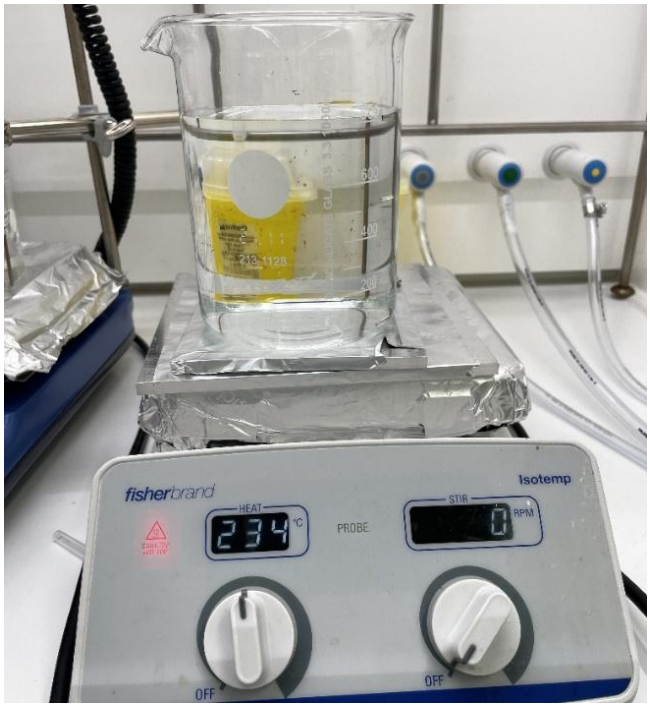

Figure 10. Polymer melting set-up.

The polymer sheets were cooled down slowly. The thickness of polymer sheets was approximately 0.2–0.4 mm. Sheets were cut into pieces with scissors that were heated on a hot plate to 80 °C. Dimensions of the cut samples were 2–4 mm x 15 mm. Samples weighed 7.6 mg ± 3.9 mg.

5.2 Hydrogen Peroxide Plasma Treatment and Gamma Irradiation

Plasma-PLGA samples were sterilized at temperature of 48 °C. The process printout received from the service provider showed that temperature in the sterilization chamber was between 49.6 °C and 51.7 °C during the process. The sterilization process duration was 20 minutes.

Gamma irradiation dose was desired to reach 25 kGy ± 10 %. Gamma ray treatment certificate received from the service provider stated dose values shown in Table 5 for the irradiation. As

can be seen, the difference between result minimum and result maximum doses is only 0.84 kGy.

Table 5. Gamma irradiation expected and result minimum and maximum doses.

Expected minimum dose (kGy)	Expected maximum dose (kGy)	Result minimum dose (kGy)	Result maximum dose (kGy)
22.50	27.5	24.63	25.47

5.3 *In Vitro* Degradation Test

In vitro degradation testing was performed on two batches of control-PLGA samples, later referred as control-A-PLGA and control-B-PLGA, and on gamma-PLGA samples (for plasma-PLGA samples, see chapter 6.1, *Hydrogen peroxide plasma sterilization)*.

Control-A-PLGA samples were placed in screw-top bottles of 4 mL individually. The bottles were rinsed with ethanol and distilled water beforehand. Samples were weighed with an analytical scale (precision of 0.1 mg) prior placing them into the bottles. 1 mL (mass by g to volume by mL ratio greater than 30:1) of 7.4 pH PBS solution (Gibco™ PBS, pH 7.4) was measured into each bottle. The samples were placed on the floor of the incubator (VWR 10055-006 INCU-Line Digital Incubator), and temperature was set to 37 °C. The degradation experiment of control-A-PLGA samples was carried out for 2 weeks, after which it was discontinued due to experimental errors.

Control-B-PLGA samples and gamma-PLGA samples were placed in Eppendorf tubes individually. The equipment used, including tweezers and a glass container for pipetting PBS, were disinfected with ethanol for 30 minutes and rinsed with distilled water before use. The samples were weighed with an analytical balance prior to placing them into the tubes. 1 mL of pH 7.4 PBS was measured into each tube, ensuring a full immersion of the samples under the solution. The tubes were placed onto an Eppendorf rack shown in Figure 11, that was placed in the incubator at 37 °C. At predetermined intervals (days 3 or 4, 7, 10, 14, 17, 21, 24 and 28), samples were imaged to determine the visible degradation process. PBS solution was changed to fresh every two weeks. The tubes were rinsed with clean PBS before measuring 1 mL of fresh PBS into them.

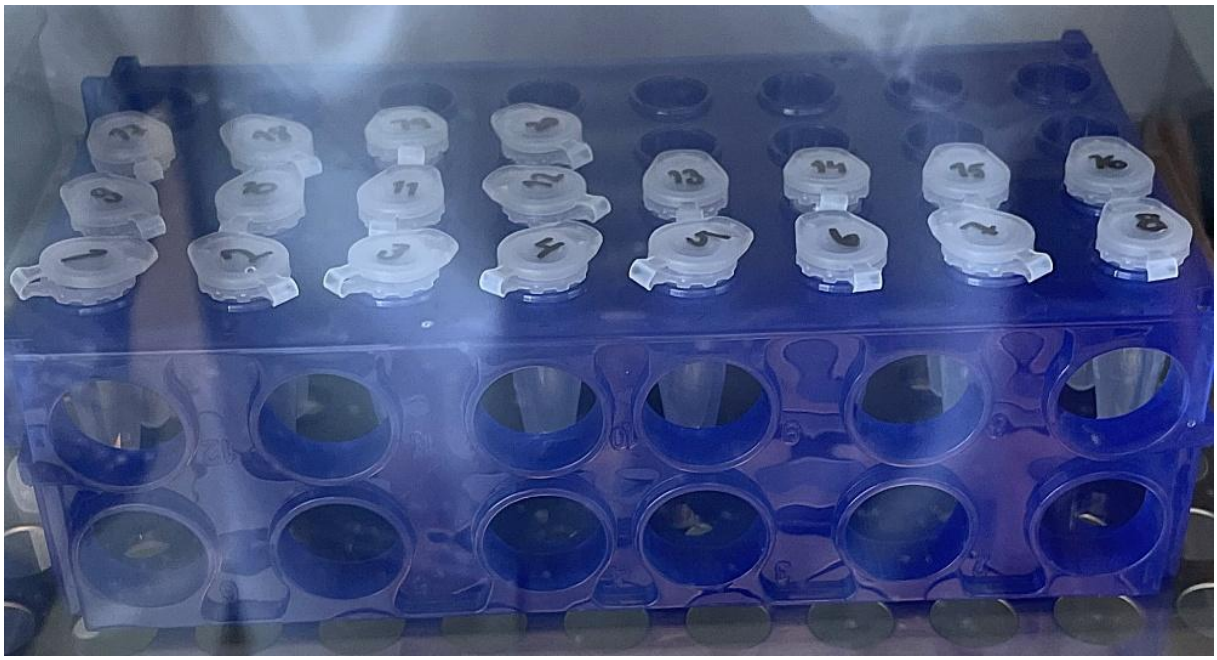

Figure 11. The unsterilized samples on the rack in the incubator.

Three gamma-PLGA samples were removed from the experiment on days 3, 7, 10, 14, 17, and 21 to determine the degradation. The samples were gently wiped with a tissue and weighed with an analytical balance for water absorption. Samples were then placed under a fume hood for one week to dry, after which they were weighed again to determine mass loss.

6 Results

The primary interest in this case focused on the degradation rate and behavior of PLGA (50DL/50G) polymer. The impact of sterilization was considered to be a critical factor, which was proven by the experiment. This chapter provides thorough insights into the results of the experiment, and observations made during the experiment that have or may have affected the results or caused errors. Each type of sample, including control-PLGA, plasma-PLGA and gamma-PLGA, were imaged with an optical microscope to reveal a close-up to the structure of these samples.

All samples were prepared by the same method, meaning that each sample looked like the control-PLGA in Figure 12 before the sterilization treatment. As can be seen on the left in Figure 12, the samples are not completely clear and see-through, but rather translucent. On the right in Figure 12 is a microscopic image of one unsterilized sample. The microscopic image revealed clear air bubbles that are densely distributed, which explains the translucency of the samples.

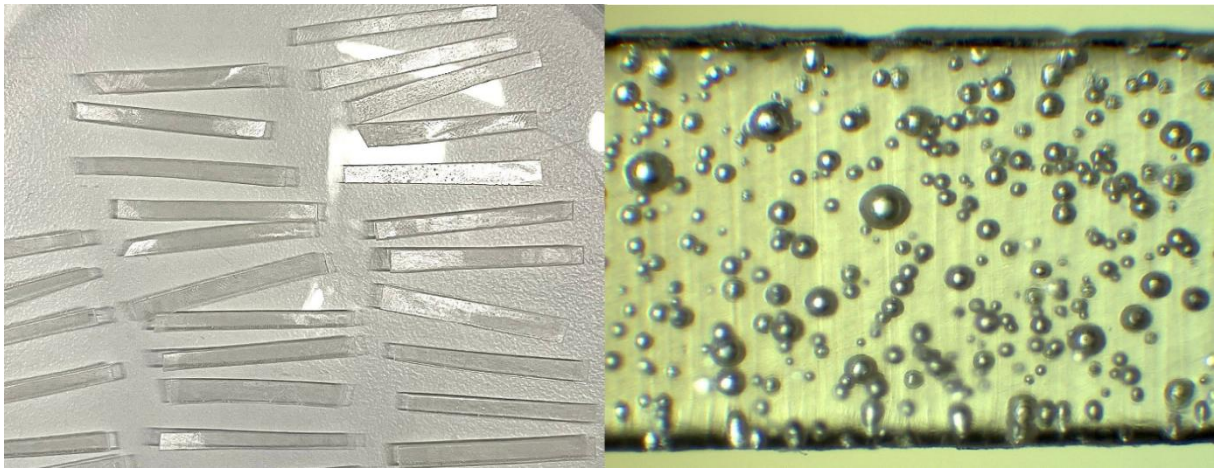

Figure 12. On the left: control-PLGA samples after fabrication. On the right: microscopic image of a control-PLGA sample, where air bubbles can be seen.

It was noted that while the hot plate was set to 236 °C (the melting point of Resomer® RG 503 H, Poly(D,L-lactide-*co*-glycolide)) during the sample fabrication, the polymer did not likely reach that same temperature. Temperature distribution on the hot plate, and the thermal conductivity of the metal plate and aluminum foil are affecting factors. It was observed that the polymer did not become liquid at any point of the melting but rather remained soft and gum-

like during the fabrication process of the polymer sheets. This means that the actual processing temperature of the polymer was much lower than its actual melting temperature.

The air bubbles are a result of air that had been trapped in between the polymer pellets while heating. Since the processing temperature did not reach the actual melting temperature of the polymer, it did not gain a complete liquid phase. Thus, air was not able to escape as the polymer pellets softened around it, which resulted in entrapment of air into the sample sheets, observed as air bubbles seen on the right in Figure 12.

The melting behavior of the polymer was further investigated later to understand the effect of temperature. The polymer pellets were heated in an oven where the temperature could be better controlled, and the heat distribution was more stable. The polymer was observed to achieve liquid state after heating for 15 minutes, while the temperature remained between 230 °C and 234 °C. This test led to complete melting of the polymer, and the polymer showed clearer and almost transparent polymer samples after cooling down and solidifying. A microscopic image of this test can be seen in Figure 13. This means that the sample preparation temperature had a significant effect on the samples that were later used to conduct the degradation studies.

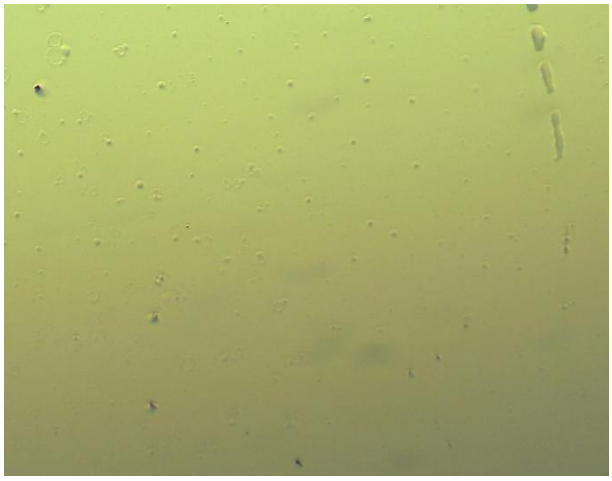

Figure 13. A microscopic image of the melting behavior test.

6.1 The Effect of Sterilization

Hydrogen peroxide plasma sterilization. The effect of hydrogen peroxide plasma sterilization method was found to be destructive on the plasma-PLGA samples. As is shown on the left in Figure 14, plasma-PLGA samples have melted together at the points where they have crossed over each other. In addition, the samples had melted onto the sterilization pouch, and they could

not be removed from the pouch without breaking them. Compared to the image on the left in Figure 12, the structure of the samples has faced significant changes. The air bubbles seem to have expanded, forming a highly porous structure. On the right in Figure 14 is a microscopic image of one plasma-PLGA sample, which illustrates better the expansion of the polymer.

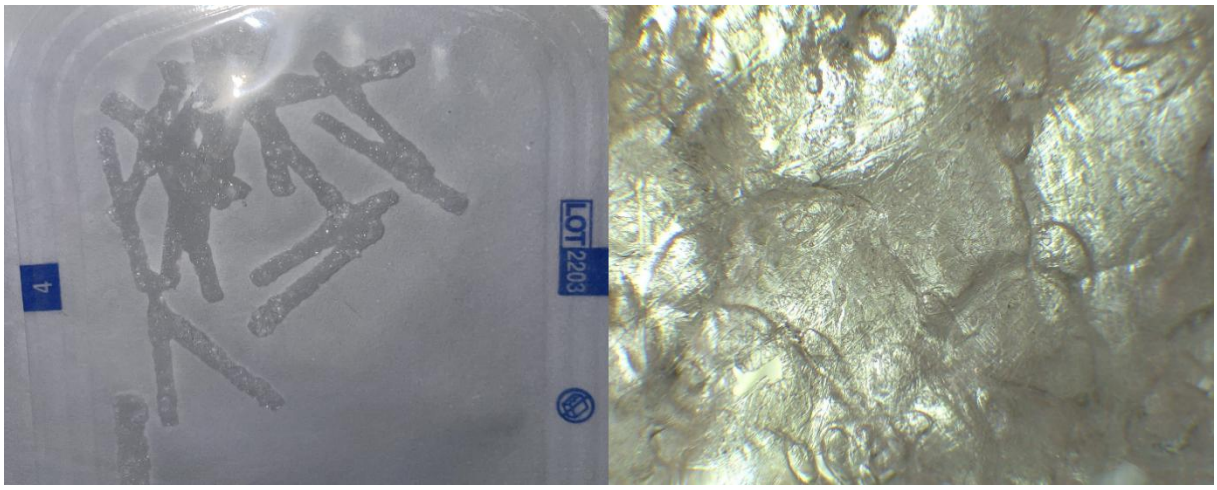

Figure 14. On the left: plasma-PLGA samples in sterilization pouch. On the right: microscopic image of a plasma-PLGA sample.

Due to structural changes and melting, plasma-PLGA samples could not be used to study the degradation. For the application of interest, the implant material should not suffer from this type of destructive effect during sterilization, as it changes the mechanical and degradability properties crucially. However, due to the fabrication errors that led to the formation of air bubbles into the samples, these plasma-PLGA samples are not comparable to the application of interest.

Gamma irradiation. Gamma-PLGA samples suffered less from sterilization than plasma-PLGA samples. On the left in Figure 15, gamma-PLGA samples can be seen. Compared to control samples on the left in Figure 12, some small changes can be seen in the gamma-PLGA samples. These samples seem to have gotten some tiny visible dots after the gamma treatment. On the right in Figure 15, a microscopic image of one gamma-PLGA sample is shown. Compared to the control samples on the right in Figure 12, the gamma samples have experienced structural changes during the irradiation process. The microscopic image on the right reveals a vague and less clear texture of the gamma sample.

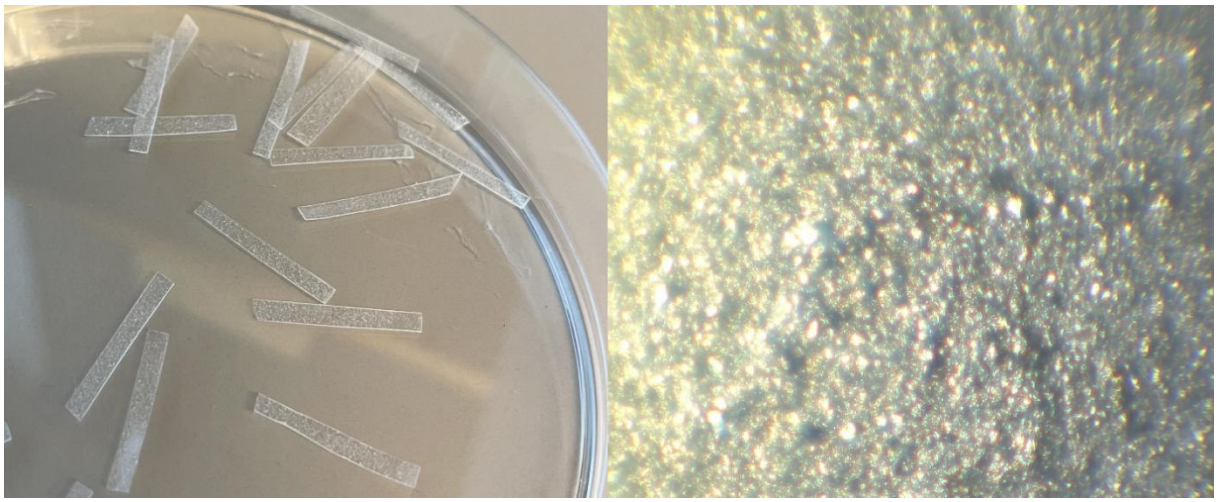

Figure 15. On the left: gamma-PLGA samples. On the right: microscopic image of a gamma-PLGA sample.

It is difficult to distinguish individual air bubbles in the microscope image of a gamma-PLGA sample, unlike in the case of control-PLGA samples. The tiny dots seen in the gamma-PLGA samples indicate that the entrapped air has slightly expanded, like in the case of H_2O_2 plasma sterilization but with significantly milder effects. Otherwise, the samples appeared to be in good condition and easy to handle, and they were qualified for degradation studies.

6.2 Hydrolytic Degradation

Unsterilized control-A-PLGA and control-B-PLGA samples were investigated, as the first round of testing with control-A-PLGA turned out to be faulty. It was observed that the control-A-PLGA samples were not degrading uniformly and much variability between different samples' degradation processes had occurred. At first, control-A-PLGA samples seemed to be degrading randomly, but after 12 days of the experiment a pattern was recognized. The samples in the screw-top bottles were placed on the floor of the incubator in four rows, five bottles each row. The first row was the nearest to the incubator door, while the last row was the innermost. The pattern had formed in a way that the samples on the first row were the least degraded, while the samples on the innermost row were almost completely degraded. Gradual degrading from the first to the innermost row can be seen in Figure 16. It is noteworthy that each row has been documented the same moment.

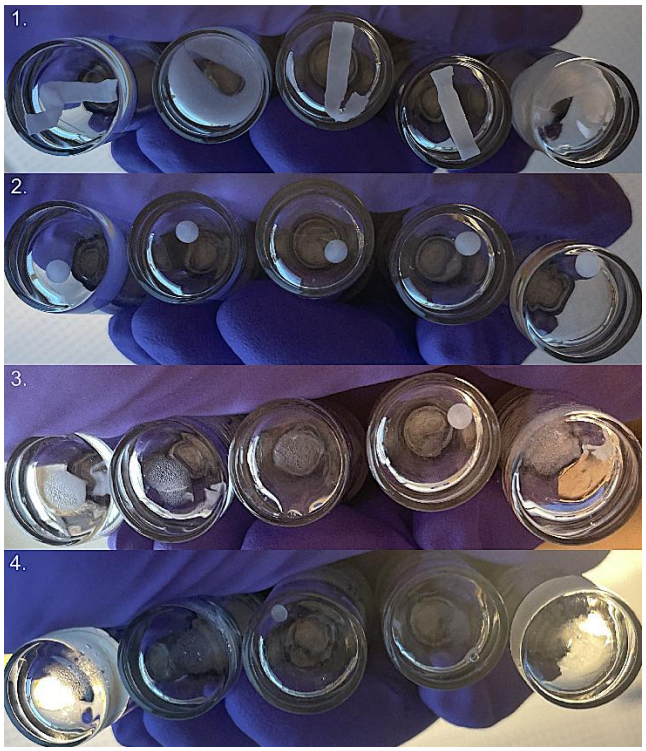

Figure 16. Gradual degradation of control-A-PLGA samples by rows.

To understand the pattern seen in Figure 16, temperature was measured with an infrared thermometer at each row from two points in the incubator, from the floor and from the top of a cap of one screw-top bottle. The temperatures observed are shown in Table 6.

Table 6. Temperatures by rows.

Row, samples	**Top of a cap**	**Incubator floor**
Row 1. samples 1–5 (closest to the door)	36 °C	35.5 °C
Row 2. samples 6–10	37.3 °C	37.5 °C
Row 3. samples 11–15	38.8 °C	38.3 °C
Row 4. samples 16–20 (the innermost)	40.7 °C	39.5 °C

It can be seen clearly from Table 6 that the temperature was not constant on the floor of the incubator. The exact desired temperature of 37 °C cannot be found in the table, and most of the temperatures are above it. Furthermore, the largest difference between temperatures is 5.2 °C.

Another error observed with some of the control-A-PLGA samples was a bizarre transformation from a strip-sample to film-like at the interface of PBS and air. It seems that the part of a sample that had got stuck in the surface tension of PBS solution had expanded forming a film, while the part of a sample that had stayed under PBS remained a strip, which can be seen in Figure 17.

Figure 17. Film formation of a control-A-PLGA sample at the interface of air and PBS, while remaining strip under the interface.

Control-B-PLGA samples experienced uniform degradation within all samples, and no film was observed. However, it was noticed that the samples stuck onto the wall and bottom of the tubes and were not freely moving in the tubes. Therefore, the control-B-PLGA samples were not exposed to PBS uniformly at all sides of the sample, as the stuck side was not in full contact with PBS. Additionally, the sticking made the samples difficult to handle, leading to a few samples breaking during the removal from the tubes. Samples were found to be fragile after the excessive PBS had been wiped out and most of the samples crumbled, which is shown in Figure 18. The crumbling made the samples difficult to handle, and they were not weighed for water absorption or mass loss. It is notable that the effects seen in Figure 18 were caused by only a very small force.

Figure 18. Broken control-B-PLGA samples after removal from PBS.

Control-B-PLGA samples were documented at certain predetermined intervals. Figure 19 shows the same samples during the degradation on days 4, 7, 10, 14, 17, 21, 24 and 28. The start date of studies was considered day 0.

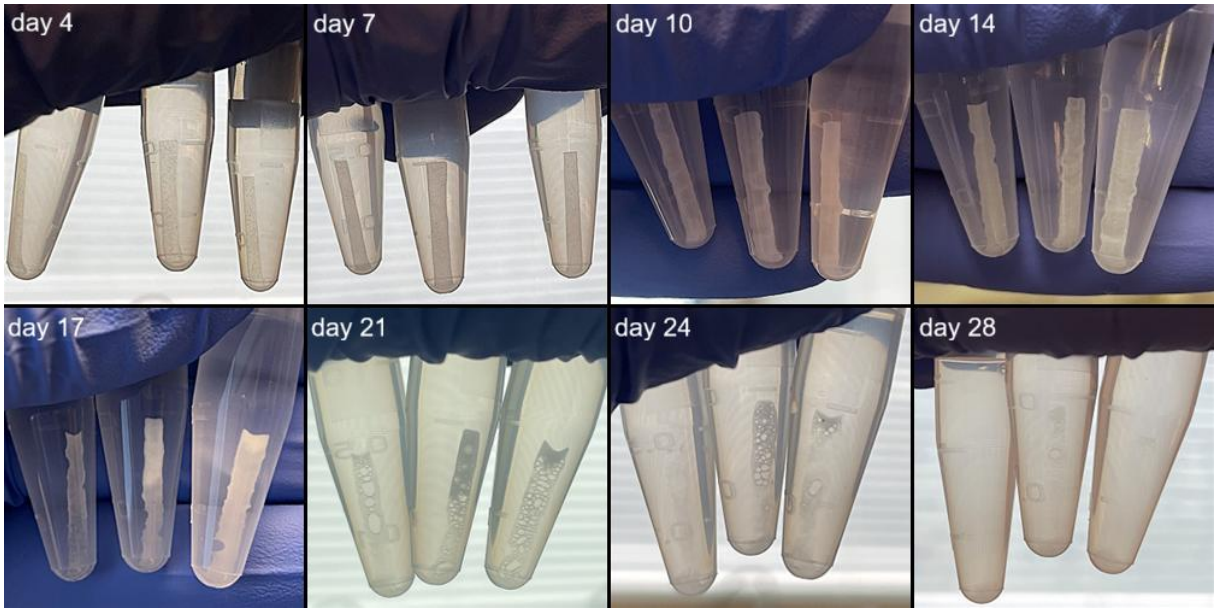

Figure 19. Degradation of unsterilized control-B-PLGA samples by days.

On days 4 and 7 of degradation, the control-B-PLGA samples are still quite translucent. On day 10, the samples have become whiter and wrinkled. This is due to the slow water absorption into the samples. On day 14, the samples are white and still well in shape. Visible degradation can be observed on day 17, which can be observed as deformations in the strips. Between days 17 and 21, rapid degradation has occurred. On day 24, very little of the samples' structures are left and no strip-shape of the samples can be clearly distinguished anymore. On day 28, two of the samples have completely degraded as there are no visible traces of them remaining, and only very little can be seen from one sample. The degradation study of the unsterilized samples was considered complete on day 28.

The gamma-PLGA samples did not experience the same type of sticking onto the walls and bottom of the tubes like the control-B-PLGA samples did, which made the samples easier to handle. The samples did not show the same type of breaking and crumbling either, as was seen in Figure 18 in the case of control-B-PLGA samples. The gamma-PLGA samples were documented at certain intervals as well. Figure 20 shows the same samples during the degradation on days 3, 7, 10, 14, 17 and 21. The start date of studies was considered day 0.

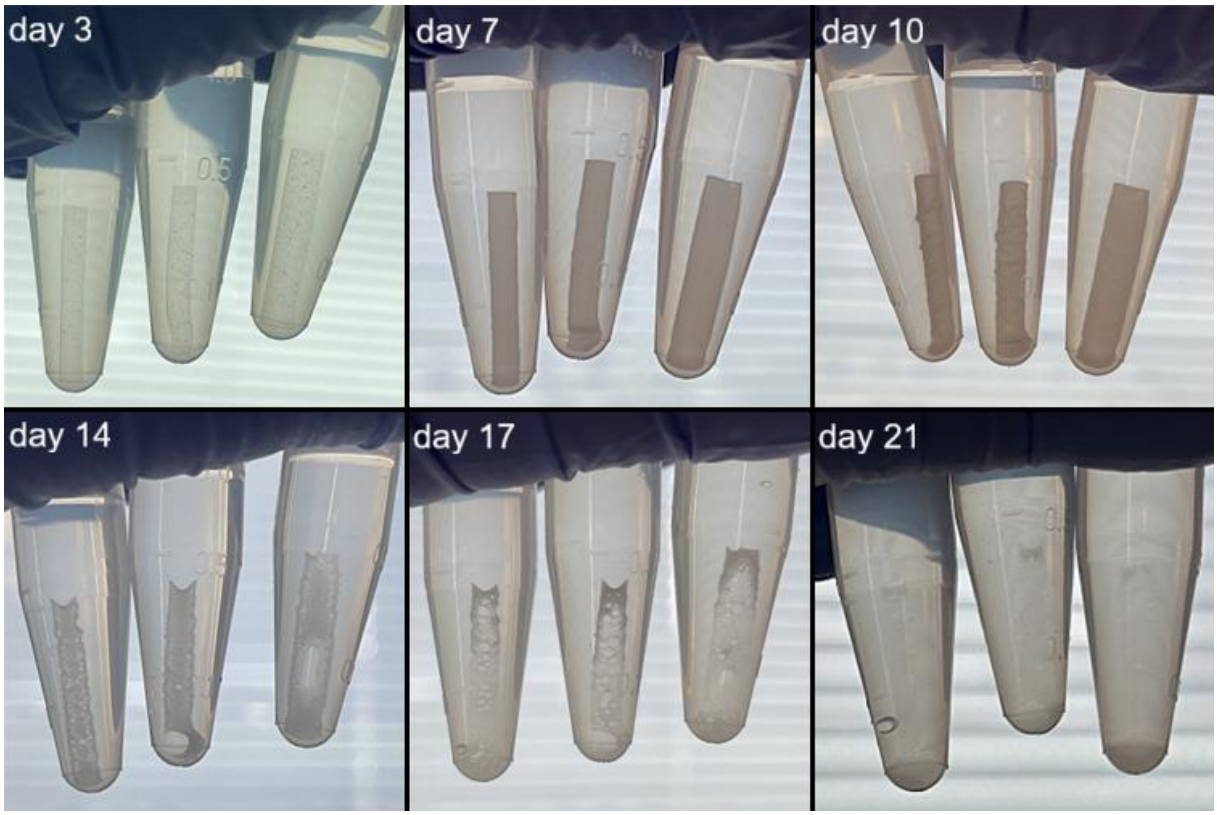

Figure 20. Degradation of gamma-PLGA samples by days.

On day 3, the gamma-PLGA samples are still translucent. On day 7, the samples have become white due to water absorption. On day 10, the samples have gained wrinkles, but no visible degradation can be detected yet. On day 14, significant changes in the samples' structures have occurred, compared to day 10. This means that a fast diffusion of monomers has started between days 10 and 14. On day 17, samples can still be detected, but on day 21, almost no trace of the samples can be visibly detected. The degradation study of gamma-PLGA samples was considered complete on day 21.

The control-B-PLGA samples started showing visible degradation on day 17, after which rapid changes were observed. The gamma-PLGA samples started showing degradation earlier than the control-B-PLGA samples, already on day 14. Visible degradation and the loss of structure of the control-B-PLGA occurred within 28 days, while in the case of gamma-PLGA the loss of structure took 21 days. Thus, it can be drawn that gamma treatment reduced degradation time about 7 days, which is 20 % less than the degradation time of the unsterilized control-B-PLGA samples.

Water absorption seems to have occurred faster in gamma-PLGA samples than in control-B-PLGA samples. Comparing day 7 of degradation between these samples, the control-B-PLGA

samples are still quite clear, while the gamma-PLGA samples are whiter. This means that more water absorption has occurred on day 7 in the gamma-PLGA samples.

6.2.1 Water Absorption

Due to the early stage breaking of a few control-B-PLGA samples after removal from PBS, those samples were excluded from water absorption and mass loss studies, and only the gamma-PLGA was investigated. Moreover, only the gamma-PLGA samples were critical in terms of water absorption and mass loss, since the implant will be sterilized. On days 3, 7, 10, 14, 17 and 21 of degradation three gamma-PLGA samples were taken out from the degradation solution and weighed to define water absorption. Water absorption(%) was calculated for each gamma-sterilized sample by equation 4, as the following example:

$$\text{Water absorption}(\%) = \frac{6.9\ \text{mg} - 5.7\ \text{mg}}{5.7\ \text{mg}} * 100\ \% = 21.05\ \%$$

The progress of water absorption during the 21 days of degradation is shown in the graph in Figure 21. Each weighing point consisted of three samples, except for day 21 where only two samples were analyzed. The mean value of the samples was used.

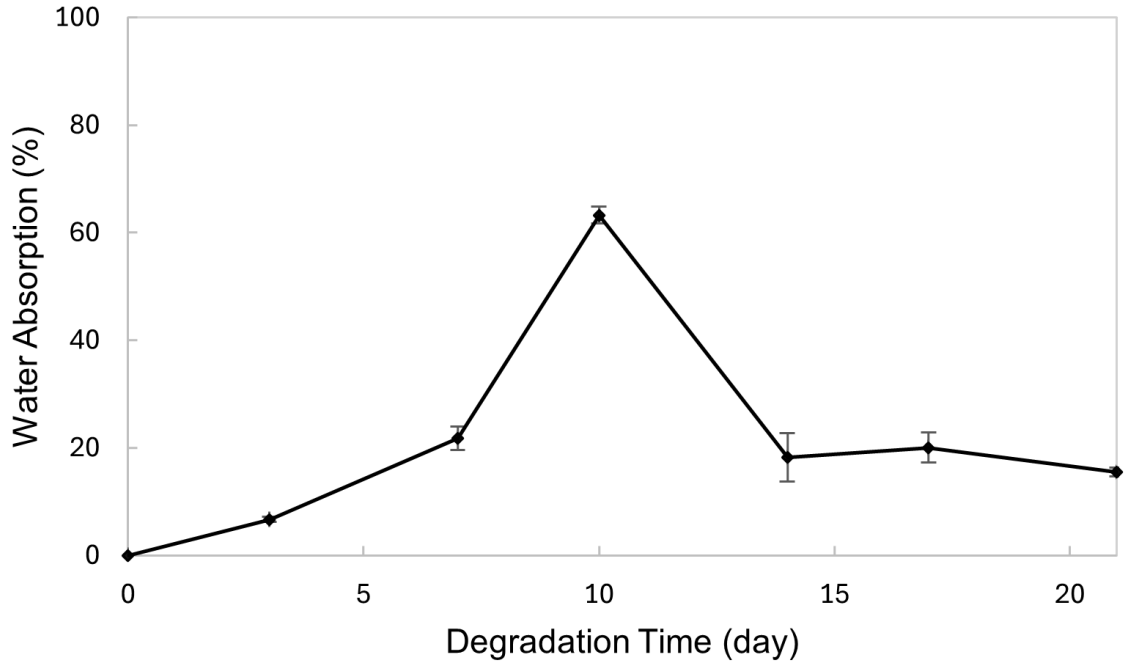

Figure 21. Water absorption of gamma-PLGA samples during the degradation.

From the graph in Figure 21 it can be seen that water absorption increased progressively until day 10. Between days 10 and 14, a rapid decrease can be observed after which the water absorption continues to decrease slowly. In Figure 20, significant changes in the gamma-PLGA samples were also reported between days 10 and 14. The transition from increased absorption capacity to decreased capacity may be a consequence of the rapid material loss, which could have resulted in less material that could retain water.

6.2.2 Mass Loss

After weighing the gamma-sterilized samples for water absorption, they were placed in a fume hood for 1 week to dry and weighed again for degradation(%). Degradation was determined by mass loss from the initial dry weight before degradation. Degradation(%) for each gamma-PLGA sample was calculated by using equation 3 as follows:

$$\text{Degradation}(\%) = \frac{7.7\ \text{mg} - 7.6\ \text{mg}}{7.7\ \text{mg}} * 100\ \% = 1.30\ \%$$

The degradation process during the 21 days can be observed in the graph in Figure 22. Each weighing point consisted of three samples, except for day 21 where only two samples were analyzed. The mean value of the samples was used.

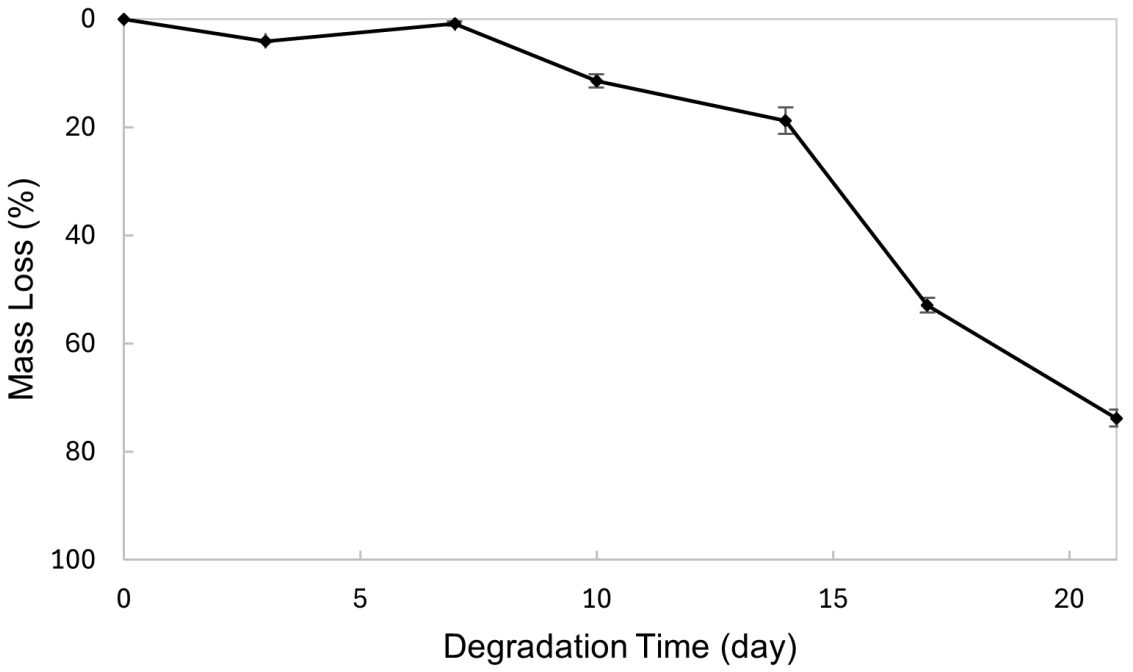

Figure 22. Mass loss of gamma-PLGA samples during the degradation.

Mass loss is progressively proceeding through the degradation time, excluding day 7 where it seems that samples have lost less mass than on the preceding weighing day. This may be due to variability in samples that were previously stated to have suffered errors in fabrication. It may also be a consequence of insufficient drying, meaning that some water had remained in the samples, which would have increased the weight. However, each sample was dried and weighed the same way, meaning that such insufficiency in drying should have occurred in each sample. Additionally, it was made sure that the weight remained constant by weighing the samples again after a few days of the first dry weighing.

The weight loss on day 21 was 71.81 % ± 2.19 %, and the remaining dry mass was 1.9 mg ± 0.1 mg (see Appendix 1). The degradation study was terminated on day 21 based on the visual examination of the physical appearance of gamma-PLGA samples, because the main focus here was to examine how long the material can hold its shape. However, based on Figure 22, approximately 25 % of the material was still remaining on day 21.

7 Discussion

In this work, the degradation behavior of PLGA (50DL/50G) (Resomer® RG 503 H, Poly(D,L-lactide-*co*-glycolide)) was studied *in vitro*. This study focused on investigating the impacts of sterilization on the degradation, as well as the visibly observable degradation process and time. These were important issues to examine because, firstly, implant material must be sterilized before implantation, and secondly, the physical examination of the degradation process revealed how long the material would be able to fulfill its intended function. The material was required to hold its structure for 4 weeks. It was estimated that the degradation time of PLGA (50DL/50G) is 1–2 months, therefore it was selected for the experimental studies. However, the experimental study revealed that the material unsterilized was able to hold its complete physical form no more than 14 days, while the material sterilized could hold its complete physical form for even shorter period of time, 10 days. Furthermore, significant errors during the laboratory work occurred, which mainly rooted to the errors made in sample preparation and the equipment setups. These errors are discussed in detail in this chapter.

All the samples were prepared into sheets by thermal processing of PLGA pellets. During the heating process, temperature did not meet the melting temperature of the polymer (T_m=236 °C), which was due to the heat transfer and conductivity of the hot plate, the metal plate and aluminium foil used in fabrication. The consequence of this was entrapment of air into the samples, which were observed as air bubbles in the microscopic image in Figure 12.

The polymer sheets were cut into strips with heated scissors. The scissors were heated over the glass transition temperature of the polymer (T_g (Resomer® RG 503 H, Poly(D,L-lactide-*co*-glycolide))=44–48 °C), so that the polymer would soften during the cutting, to achieve a smoother cut and minimize any cracking of the brittle polymer sheet. However, minor cracks may still have been formed in the samples, which would not have been visible by the bare eye. These cracks would have allowed better water penetration into the polymer structure, which would in turn affect the degradation rate. Additionally, when some of the unsterilized samples crumbled after removing them from PBS, it may be a consequence of these small cracks. Furthermore, variation between samples may have occurred, as the cutting was performed by hand, which may have resulted in variable cut profiles.

In the case of unsterilized control-A-PLGA samples, a film formation at the interface of PBS solution and air was observed, while the end of the sample which had been under PBS still

remained a strip (Figure 17). In the case of control-B-PLGA samples, the smaller volume and shape of the 1.5 mL Eppendorf tubes ensured complete immersion of the samples in PBS solution. The 4 mL screw-top bottles did not ensure that, as the measured 1 mL of PBS did not completely cover each sample, leaving some of the samples partly floating at the surface of PBS.

The control-A-PLGA samples suffered from uneven degradation, which led to them not being qualified for the degradation study. Uneven degradation occurred mainly due to significant temperature differences from the set temperature of 37 °C and temperature differences between the sample rows. A clear correlation between Figure 16 and Table 6 was identified, which leads to a conclusion that the primary reason is, in fact, the temperature differences. In the case of control-A-PLGA samples the lowest temperature measured was 35.5 °C while the highest temperature was 40.7 °C, and the largest temperature difference measured from the incubator was 5.2 °C. As temperature increases, it enables better movement of polymer chains, which allows better water penetration into the polymer structure. Furthermore, the hydrolytic reaction rate is increased by a higher temperature. These effects lower the degradation time as temperature increases.

Moreover, the previously discussed is supported by the control-B-PLGA samples that did not experience such variations. The changes made in the degradation test arrangements for the control-B-PLGA batch ensured more stable temperature and more uniform immersion of samples in PBS solution. The changes included the use of 1.5 mL Eppendorf tubes instead of 4 mL screw-top bottles and the use of Eppendorf rack instead of placing the samples on the floor of the incubator floor. In the case of control-B-PLGA samples, the Eppendorf rack allowed better air flow in the incubator between the tubes and walls, as well as between individual tubes. To keep temperature steady everywhere in the incubator, air flow must be efficient enough. The heating elements, which were located behind the walls of the incubator were also responsible for the uneven temperatures on the floor of the incubator, where the control-A-PLGA samples were placed. The Eppendorf rack was positioned so that there was no direct contact with the heating elements.

The control-B-PLGA samples showed steady and uniform degradation. Visible degradation as a loss of physical structure was observed on day 17 of the experiment (Figure 19). This proves that the polymer undergoes bulk degradation, since it had experienced degradation by mass loss and water absorption during the first 14 days, but showed no visible degradation. Visibly

detectable degradation was observed quickly after the 14 days point, which was a result of sufficient molecular weight loss for the monomers to burst and diffuse out.

Hydrogen peroxide plasma sterilization resulted in destructive effects in the polymer. Based on literature, this was expected, as the free hydroxyl radicals formed during the H_2O_2 plasma sterilization process may cause changes in in the chemical structure [55]. The plasma-PLGA samples gained visibly porous structure, and they had melted together as well as onto the sterilization pouch. This was likely due to the entrapped air found in the samples in microscopic examination. It seems that the polymer had allowed those air bubbles to expand during the sterilization process, after which the polymer solidified in the expanded state. H_2O_2 plasma sterilization was done at 48 °C, while the glass transition temperature of Resomer® RG 503 H, Poly(D,L-lactide-*co*-glycolide) is 44–48 °C. Sterilization temperature was thus just above the polymer's T_g. Above that T_g, the polymer transforms into softer and more flexible state. At the same, the growing pressure caused by the higher temperature forced the air bubbles to expand. Since the polymer had reached a soft and flexible state, it allowed expansion.

Based on the experiment performed, H_2O_2 plasma treatment is destructive to PLGA (50DL/50G). However, there are studies arguing that hydrogen peroxide plasma treatment could be well suitable for biodegradable polymers, because it is not structurally destructive and it is effective at sterilizing, while it does not leave toxic residuals either [54, 55, 58, 68]. In this case, the cause of the destructive effects was found to be a result of the sample fabrication process. For this reason, the results of the experiment are not reliable, and no further conclusions can be drawn based on them. For further investigation and reliable results, the samples should be prepared in a way that the polymer melts completely, leaving no entrapped air in. That is, the actual temperature of the polymer during sample fabrication process should reach its melting point (236 °C). In that manner, the samples would be more representative of the implant, as the material is intended to be throughout solid and not porous. Additionally, the H_2O_2 plasma sterilization should be conducted at temperature lower than the glass transition temperature of the polymer. However, the lower treatment temperature acquires longer treatment time as well, which should be considered as well.

Gamma-sterilization effects appeared to be milder than those of H_2O_2 plasma treatment, based on the experiment. Shape of the gamma-PLGA samples remained visibly the same as before the treatment, but the microscopic imaging revealed that some structural alterations had occurred (Figure 15 vs. Figure 12). The changes in structure and appearance may have been a

result of the high energy of gamma rays, that may have led to destructive structural effects like chain cleavage, crosslinking or oxidation [9]. It is known that biodegradable polymers are more sensitive to sterilization effects, and they are typically more susceptible to bond cleavage by high energy rays than nondegradable polymers [55]. Furthermore, as the temperature during the gamma irradiation process is not controlled and may reach up to 40 °C [9], the effect of temperature cannot be neglected. Although the temperature was lower than that used in H_2O_2 plasma treatment, and lower than the T_g of the polymer (48 °C), it should be noted that the service provider did not specify any temperature control.

Wrinkles appeared in both control-B-PLGA and gamma-PLGA samples over the first 3 days of imaging. Vey et al. suggested that the wrinkling results from swelling of an outer layer that has been formed at the surface of the sample [69]. Interestingly, they compared this event to fingertips that have been soaked under water for a long time [69]. Vey et al. presented that over the first days of PLGA (50/50)'s degradation the surface layer of a sample absorbs a great amount of water and swells significantly [69]. At the same time, a phenomenon called autocatalysis is taking place inside the bulk [69]. Autocatalysis happens when the degraded oligomers with acidic moieties form more acidic conditions in the bulk of the polymer as they cannot diffuse efficiently out yet, while the degrading oligomers at the surface are able to escape and be neutralized [70]. The acidic monomers and oligomers enhance degradation inside the polymer, which causes faster degradation inside the bulk of the material than on the surface [70].

Water absorption was likely assisted by the air bubbles in the samples. This can be observed on days 21 and 24 of control-B-PLGA samples' degradation (Figure 19), and on days 14 and 17 of gamma-PLGA samples' degradation (Figure 20). On those days, both of the sample types were significantly porous and fragmented. This is because the degradation has proceeded from the bubbles. The air bubbles increased the surface area from which water was absorbed into the polymer sample. However, the surface area-to-volume ratio should not possess drastic effects on the degradation rate in case of bulk degradation. Because bulk degradation was identified to be the degradation mechanism of PLGA (50DL/50G), the entrapped air should not have had a major impact on the hydrolytic degradation time in that manner.

As it was observed through the degradation images (Figures 19 and 20), gamma treatment significantly impacted the degradation time by reducing it by about 20 %. No visible traces could be observed in the control-B-PLGA samples after 28 days, while the gamma-PLGA

samples were detectable for only 21 days. The previously discussed effect of gamma irradiation causing chain scission is likely the reason. High energy of the gamma rays caused undesired chain cleavage to the polymer network, which lowered the degradation time. These results are important, because the implant will be sterilized, and the effect of sterilization must be considered. The degradation time of a material stated in literature usually refers to the plain material, and it does not necessarily consider any processing phases or the effect of sterilization. In the case of implants, sterilization is however critical.

In the gamma-PLGA's water absorption graph (Figure 21), the absorption progressively increased to day 10, after which the absorption percentage dropped. From the degradation images (Figure 20), after day 10 the structure of the samples had become porous, and rapid degradation was detected. Water absorption was the highest just before the formation of pores, i.e., before the monomers and oligomers could diffuse out. When the molecular weight of polymer chains at the surface had decreased enough, degraded parts could escape and the water containing capacity of the polymer decreased.

An obvious mass loss of the gamma-PLGA samples began after day 7 (Figure 21), and continued relatively slowly until day 14, after which more rapid degradation was seen. Degradation images (Figure 20) showed that on day 21, there was no structure left, while according to the mass loss figure, about 25 % of the mass was still remaining that same day. At that point, the length of the polymer chains had decreased to a point where they could no longer hold and show a clear shape, but the polymer had still not completely degraded yet.

7.1 Material Selection

The unsterilized material was capable of holding its complete physical shape for 14 days, after which a rapid degradation occurred, while the gamma-sterilized material was capable of holding its complete physical shape only for 10 days. Nevertheless, both the control-B-PLGA and gamma-PLGA showed shorter degradation time than what is required for the case. With that being said, the material PLGA (50DL/50G) is not applicable according to the laboratory testing. The selected material should have a longer degradation time, during which the shape should be held for 4 weeks.

It should be pointed out that the reported degradation time of a material does not directly indicate how long that material is capable of fulfilling its function by holding its shape. This was observed in the results (Figure 20 vs. Figure 22), where there was mass remaining still on

day 21, while no shape or structure could visibly be seen. The intended use of biodegradable material must be considered thoroughly, because different purposes require significantly different performance in terms of biodegradation. As an example, a drug delivery system is most likely to primarily rely on steady degradation, during which therapeutic agents are released consistently throughout the degradation until the last part of material is degraded. On the other hand, an implant that does not primarily or at all release therapeutic agents is most likely required to hold a specific functional shape until a certain point, after which the functionality of the device is lost. The requirements for these different types of implants vary greatly in terms of their degradation profile.

7.2 Future Work

As was stated, poly(D,L-lactide-*co*-glycolide) with copolymer ratio of 50/50 experienced faster *in vitro* hydrolytic degradation than was expected, and thus it is not suitable for the application of interest. The gamma-sterilized material did not maintain its complete physical shape after day 10 of the studies, while it is required to do so for 4 weeks. Fortunately, there are a variety of factors that have an impact on the degradation process and time of PLGA, and the opportunities for alterations and tuning are wide. Not only can its degradation be modified in terms of copolymer ratio, but also by the molecular weight and end groups. Altering the copolymer ratio is suitable for larger modifications, while the end groups and molecular weight can be used for fine tuning. Therefore, the focus in future studies should be on changing the copolymer ratio, which has a more pronounced impact on degradation to achieve a notably lower degradation rate. The addition of either lactide or glycolide will increase the degradation time, since the ratio of 50/50 of lactide and glycolide has the fastest degradation rate. However, the ratio should be kept under 85L/15G, which has degradation time of 12–18 months [29].

Future work should be done in a way that ensures no similar mistakes and errors as presented in this thesis are repeated. Firstly, the importance of a good laboratory notes keeping should not be overlooked. In fact, consistent note keeping during this work enabled the tracking of errors. The most outstanding errors can be avoided by using the melting temperature in sample preparation, immersing the samples fully under PBS solution, and keeping sufficient airflow around the samples. Also, for better comparison both unsterilized and sterilized material should be tested for mass loss and water absorption, and the tests should be done similarly. Furthermore, the effect of sterilization on mechanical properties should be investigated.

Although the shape memory effect was not further examined and tested in this thesis, it still holds great opportunities for the future. Shape memory could be utilized to assist the insertion of the implant, which could be done through a minimally invasive cut. The T_{trans} of the SMP should be close to the human body temperature 37 °C, so that the memory effect would be activated upon implantation. This way the implant would be easy to deliver to the body with minimal intervention, and the implant would reach its functionality when introduced to body temperature. Thus, SMPs possess great potentials in addressing certain challenges that may be faced in this case. Previously presented triblock PLGA/PCL/PLGA and PLCL50/PLGA50 are some potential copolymers, which could be investigated more. For future work, the shape memory effect should be explored in regards of transition temperature, degradability, and shape fixity and recovery rates.

However, shape memory polymers usually consist of at least two different polymers, which may require more investigation and studies. It must be noted that while the individual polymers used for shape memory may be considered biologically safe and may have FDA and MDR approvals, that may not be the case for their blends or mixtures. Polymer blends are generally considered to be completely different materials, and their combination must be assessed as an individual material. This can pose challenges when addressing biocompatibility, degradation pathways and rate, mechanical properties and functionality. Additionally, considering the price of the polymers versus the benefit of the property, the utilization of shape memory polymers must be evaluated. Shape memory property requires at least three additional processing steps, including heating, shaping and cooling, which increase the implant's manufacturing costs. In addition, the cost of two polymers may be higher than the cost of one.

8 Conclusions

In this work, the material for a biodegradable intravenous implant was examined. To meet the requirement of rapid degradation time, the focus was pointed to biodegradable polymers, more specifically to polyesters, which are the most employed polymers in similar applications, stents. PLA, PGA, PLGA and PCL are aliphatic polyesters, that were considered for the case. PLGA (50DL/50G) appeared to be the most suitable in terms of short degradation time, which had been reported to be 1–2 months. The laboratory experiment performed in this work showed that PLGA (50DL50G) (acid terminated, M_w=24,000–38,000) could retain its complete physical form for 14 days and had lost its visible structure completely within 28 days. The same material treated with gamma irradiation for sterilization could retain its complete physical form for only 10 days and had lost its visible structure completely within 21 days. As it was determined that the structure of the material should remain for 4 weeks, this material was ultimately confirmed to be unsuitable.

The final material selection process should be continued in future studies, based on the knowledge gained from this thesis. It was suggested that the focus should be pointed to altering the copolymer ratio, to achieve longer degradation time. However, the ratio should be less than 85/15 of lactide and glycolide. Factors that affect the degradation time, such as manufacturing process and sterilization, should also be thoroughly considered. In fact, the effect of sterilization is critical to acknowledge, since the implant will be sterilized. Moreover, end groups and molecular weight of the polymer are additional affecting factors in degradation rate, which should be paid attention to.

While the material properties are the baseline of selecting a suitable option, the degradation time is also impacted by processing and post-processing. The manufacturing process of the implant may cause polymer degradation or other destructive effects if high temperatures are used. As the experimental section showed, sterilization also significantly lowers the degradation time. Different sterilization methods have variable effects, but all together it can be stated that the effects are nearly always negative. The effect of sterilization on degradation should thus always be considered and examined.

Lastly, the impact of sterilization on the material's mechanical properties and the their loss progression during the hydrolytic degradation of the polymer should be investigated. The most

important properties include tensile strength, compression strength and flexural properties. The importance of defining these characteristics is based on the functionality of the implant.

References

[1] D. B. Camasão and D. Mantovani, "The mechanical characterization of blood vessels and their substitutes in the continuous quest for physiological-relevant performances. A critical review," *Mater. Today Bio*, vol. 10, p. 100106, Mar. 2021, doi: 10.1016/j.mtbio.2021.100106.

[2] C.-H. Mi, X.-Y. Qi, Y.-W. Zhou, Y.-W. Ding, D.-X. Wei, and Y. Wang, "Advances in medical polyesters for vascular tissue engineering," *Discov. Nano*, vol. 19, no. 1, p. 125, Aug. 2024, doi: 10.1186/s11671-024-04073-x.

[3] M. A. Seidman, R. F. Padera, and F. J. Schoen, "2.5.2B - Cardiovascular Medical Devices: Stents, Grafts, Stent-Grafts and Other Endovascular Devices," in *Biomaterials Science (Fourth Edition)*, W. R. Wagner, S. E. Sakiyama-Elbert, G. Zhang, and M. J. Yaszemski, Eds., Academic Press, 2020, pp. 1033–1050. doi: 10.1016/B978-0-12-816137-1.00068-4.

[4] C. V. C. Bouten, P. Y. W. Dankers, A. Driessen-Mol, S. Pedron, A. M. A. Brizard, and F. P. T. Baaijens, "Substrates for cardiovascular tissue engineering," *Adv. Drug Deliv. Rev.*, vol. 63, no. 4, pp. 221–241, Apr. 2011, doi: 10.1016/j.addr.2011.01.007.

[5] H. Y. Ang, Y. Y. Huang, S. T. Lim, P. Wong, M. Joner, and N. Foin, "Mechanical behavior of polymer-based vs. metallic-based bioresorbable stents," *J. Thorac. Dis.*, vol. 9, no. Suppl 9, pp. S923–S934, Aug. 2017, doi: 10.21037/jtd.2017.06.30.

[6] L. Wang, L. Jiao, S. Pang, P. Yan, X. Wang, and T. Qiu, "The Development of Design and Manufacture Techniques for Bioresorbable Coronary Artery Stents," *Micromachines*, vol. 12, no. 8, Art. no. 8, Aug. 2021, doi: 10.3390/mi12080990.

[7] M. Stevanovic and D. Uskokovic, "Poly(lactide-co-glycolide)-based Micro and Nanoparticles for the Controlled Drug Delivery of Vitamins," *Curr. Nanosci.*, vol. 5, no. 1, pp. 1–14, Feb. 2009, doi: 10.2174/157341309787314566.

[8] C. E. Holy, C. Cheng, J. E. Davies, and M. S. Shoichet, "Optimizing the sterilization of PLGA scaffolds for use in tissue engineering," *Biomaterials*, vol. 22, no. 1, pp. 25–31, Jan. 2000, doi: 10.1016/S0142-9612(00)00136-8.

[9] L. Davison, E. Themistou, F. Buchanan, and E. Cunningham, "Low temperature gamma sterilization of a bioresorbable polymer, PLGA," *Radiat. Phys. Chem.*, vol. 143, pp. 27–32, Feb. 2018, doi: 10.1016/j.radphyschem.2017.09.009.

[10] L. Ghasemi-Mobarakeh, D. Kolahreez, S. Ramakrishna, and D. Williams, “Key terminology in biomaterials and biocompatibility,” *Curr. Opin. Biomed. Eng.*, vol. 10, pp. 45–50, Jun. 2019, doi: 10.1016/j.cobme.2019.02.004.

[11] A. Hudecki, G. Kiryczyński, and M. J. Łos, “Chapter 7 - Biomaterials, Definition, Overview,” in *Stem Cells and Biomaterials for Regenerative Medicine*, M. J. Łos, A. Hudecki, and E. Wiecheć, Eds., Academic Press, 2019, pp. 85–98. doi: 10.1016/B978-0-12-812258-7.00007-1.

[12] M. Jurak, A. E. Wiącek, A. Ładniak, K. Przykaza, and K. Szafran, “What affects the biocompatibility of polymers?,” *Adv. Colloid Interface Sci.*, vol. 294, p. 102451, Aug. 2021, doi: 10.1016/j.cis.2021.102451.

[13] D. F. Williams, “On the mechanisms of biocompatibility,” *Biomaterials*, vol. 29, no. 20, pp. 2941–2953, Jul. 2008, doi: 10.1016/j.biomaterials.2008.04.023.

[14] D. Pappalardo, T. Mathisen, and A. Finne-Wistrand, “Biocompatibility of Resorbable Polymers: A Historical Perspective and Framework for the Future,” *Biomacromolecules*, vol. 20, no. 4, pp. 1465–1477, Apr. 2019, doi: 10.1021/acs.biomac.9b00159.

[15] J. Bergan and L. Pascarella, “CHAPTER 4 - Venous Anatomy, Physiology, and Pathophysiology,” in *The Vein Book*, J. J. Bergan, Ed., Burlington: Academic Press, 2007, pp. 39–45. doi: 10.1016/B978-012369515-4/50007-7.

[16] J.-P. Barral and A. Croibier, “1 - General organization of the cardiovascular system,” in *Visceral Vascular Manipulations*, J.-P. Barral and A. Croibier, Eds., Oxford: Churchill Livingstone, 2011, pp. 3–26. doi: 10.1016/B978-0-7020-4351-2.00001-6.

[17] S. R. Hanson, E. I. Tucker, and R. A. Latour, “2.2.6 - Blood Coagulation and Blood–Material Interactions,” in *Biomaterials Science (Fourth Edition)*, W. R. Wagner, S. E. Sakiyama-Elbert, G. Zhang, and M. J. Yaszemski, Eds., Academic Press, 2020, pp. 801–812. doi: 10.1016/B978-0-12-816137-1.00052-0.

[18] Y. Shen *et al.*, “Development of Biodegradable Polymeric Stents for the Treatment of Cardiovascular Diseases,” *Biomolecules*, vol. 12, no. 9, Art. no. 9, Sep. 2022, doi: 10.3390/biom12091245.

[19] T. Melnik, O. Jordan, J.-M. Corpataux, F. Delie, and F. Saucy, “Pharmacological prevention of intimal hyperplasia: A state-of-the-art review,” *Pharmacol. Ther.*, vol. 235, p. 108157, Jul. 2022, doi: 10.1016/j.pharmthera.2022.108157.

[20] C. Mukherjee *et al.*, “Recent advances in biodegradable polymers – Properties, applications and future prospects,” *Eur. Polym. J.*, vol. 192, p. 112068, Jun. 2023, doi: 10.1016/j.eurpolymj.2023.112068.

[21] J. Kurowiak, T. Klekiel, and R. Będziński, “Biodegradable Polymers in Biomedical Applications: A Review—Developments, Perspectives and Future Challenges,” *Int. J. Mol. Sci.*, vol. 24, no. 23, Art. no. 23, Jan. 2023, doi: 10.3390/ijms242316952.

[22] L. Macdougall, H. Culver, C.-C. Lin, C. Bowman, and K. Anseth, “1.3.2F - Degradable and Resorbable Polymers,” in *Biomaterials Science (Fourth Edition)*, W. R. Wagner, S. E. Sakiyama-Elbert, G. Zhang, and M. J. Yaszemski, Eds., Academic Press, 2020, pp. 167–190. doi: 10.1016/B978-0-12-816137-1.00015-5.

[23] H. Y. Ang, H. Bulluck, P. Wong, S. S. Venkatraman, Y. Huang, and N. Foin, “Bioresorbable stents: Current and upcoming bioresorbable technologies,” *Int. J. Cardiol.*, vol. 228, pp. 931–939, Feb. 2017, doi: 10.1016/j.ijcard.2016.11.258.

[24] J. Zong, Q. He, Y. Liu, M. Qiu, J. Wu, and B. Hu, “Advances in the development of biodegradable coronary stents: A translational perspective,” *Mater. Today Bio*, vol. 16, p. 100368, Dec. 2022, doi: 10.1016/j.mtbio.2022.100368.

[25] S. H. Im, D. H. Im, S. J. Park, Y. Jung, D.-H. Kim, and S. H. Kim, “Current status and future direction of metallic and polymeric materials for advanced vascular stents,” *Prog. Mater. Sci.*, vol. 126, p. 100922, May 2022, doi: 10.1016/j.pmatsci.2022.100922.

[26] L. N. Woodard and M. A. Grunlan, “Hydrolytic Degradation and Erosion of Polyester Biomaterials,” *ACS Macro Lett.*, vol. 7, no. 8, pp. 976–982, Aug. 2018, doi: 10.1021/acsmacrolett.8b00424.

[27] D. da Silva *et al.*, “Biocompatibility, biodegradation and excretion of polylactic acid (PLA) in medical implants and theranostic systems,” *Chem. Eng. J.*, vol. 340, pp. 9–14, May 2018, doi: 10.1016/j.cej.2018.01.010.

[28] L. S. Nair and C. T. Laurencin, “Biodegradable polymers as biomaterials,” *Prog. Polym. Sci.*, vol. 32, no. 8, pp. 762–798, Aug. 2007, doi: 10.1016/j.progpolymsci.2007.05.017.

[29] H. Y. Ang *et al.*, “5 - Fundamentals of bioresorbable stents,” in *Functionalised Cardiovascular Stents*, J. G. Wall, H. Podbielska, and M. Wawrzyńska, Eds., Woodhead Publishing, 2018, pp. 75–97. doi: 10.1016/B978-0-08-100496-8.00005-6.

[30] B. M. Stanetic, J. Iqbal, Y. Onuma, and P. W. Serruys, “Novel bioresorbable scaffolds technologies: current status and future directions,” *Minerva Cardioangiol.*, vol. 63, no. 4, pp. 297–315, Aug. 2015.

[31] C. V. Bourantas, Y. Zhang, V. Farooq, H. M. Garcia-Garcia, Y. Onuma, and P. W. Serruys, "Bioresorbable Scaffolds: Current Evidence and Ongoing Clinical Trials," *Curr. Cardiol. Rep.*, vol. 14, no. 5, pp. 626–634, Oct. 2012, doi: 10.1007/s11886-012-0295-5.

[32] H. Qiu *et al.*, "Short-term safety and effects of a novel fully bioabsorable poly-L-lactic acid sirolimus-eluting stents in porcine coronary arteries," *Chin. Med. J. (Engl.)*, vol. 126, no. 6, p. 1183, Mar. 2013, doi: 10.3760/cma.j.issn.0366-6999.20123098.

[33] C.-I. Kwon *et al.*, "Mechanical properties and degradation process of biliary self-expandable biodegradable stents," *Dig. Endosc.*, vol. 33, no. 7, pp. 1158–1169, 2021, doi: 10.1111/den.13916.

[34] C. Martins, F. Sousa, F. Araújo, and B. Sarmento, "Functionalizing PLGA and PLGA Derivatives for Drug Delivery and Tissue Regeneration Applications," *Adv. Healthc. Mater.*, vol. 7, no. 1, p. 1701035, 2018, doi: 10.1002/adhm.201701035.

[35] Y. Huang *et al.*, "3D printing of biodegradable polymer vascular stents to treat cardiovascular diseases: A review," *Addit. Manuf.*, vol. 111, p. 104984, Aug. 2025, doi: 10.1016/j.addma.2025.104984.

[36] J. A. D. Sequeira, A. C. Santos, J. Serra, F. Veiga, and A. J. Ribeiro, "Poly(lactic-*co*-glycolic acid) (PLGA) matrix implants," in *Nanostructures for the Engineering of Cells, Tissues and Organs*, A. M. Grumezescu, Ed., William Andrew Publishing, 2018, pp. 375–402. doi: 10.1016/B978-0-12-813665-2.00010-7.

[37] L. Singh, V. Kumar, and B. D. Ratner, "Generation of porous microcellular 85/15 poly (dl-lactide-co-glycolide) foams for biomedical applications," *Biomaterials*, vol. 25, no. 13, pp. 2611–2617, Jun. 2004, doi: 10.1016/j.biomaterials.2003.09.040.

[38] J. W. Drelich and J. Goldman, "Bioresorbable vascular metallic scaffolds: Current status and research trends," *Curr. Opin. Biomed. Eng.*, vol. 24, p. 100411, Dec. 2022, doi: 10.1016/j.cobme.2022.100411.

[39] J. Iqbal, Y. Onuma, J. Ormiston, A. Abizaid, R. Waksman, and P. Serruys, "Bioresorbable scaffolds: rationale, current status, challenges, and future," *Eur. Heart J.*, vol. 35, no. 12, pp. 765–776, Mar. 2014, doi: 10.1093/eurheartj/eht542.

[40] B. Gundogan, A. Tan, Y. Farhatnia, M. S. Alavijeh, Z. Cui, and A. M. Seifalian, "Bioabsorbable Stent Quo Vadis: A Case for Nano-Theranostics," *Theranostics*, vol. 4, no. 5, pp. 514–533, Feb. 2014, doi: 10.7150/thno.8137.

[41] E. Malikmammadov, T. E. Tanir, A. Kiziltay, V. Hasirci, and N. Hasirci, “PCL and PCL-based materials in biomedical applications,” *J. Biomater. Sci. Polym. Ed.*, vol. 29, no. 7–9, pp. 863–893, Jun. 2018, doi: 10.1080/09205063.2017.1394711.

[42] G. I. Peterson, A. V. Dobrynin, and M. L. Becker, “Biodegradable Shape Memory Polymers in Medicine,” *Adv. Healthc. Mater.*, vol. 6, no. 21, p. 1700694, 2017, doi: 10.1002/adhm.201700694.

[43] R. Xiao and W. M. Huang, “Heating/Solvent Responsive Shape-Memory Polymers for Implant Biomedical Devices in Minimally Invasive Surgery: Current Status and Challenge,” *Macromol. Biosci.*, vol. 20, no. 8, p. 2000108, 2020, doi: 10.1002/mabi.202000108.

[44] K. Wang, L. Man, M. Zhang, Y.-G. Jia, and X. X. Zhu, “Programmable polymers with shape memory for biomedical applications,” *Program. Mater.*, vol. 1, p. e2, Jan. 2023, doi: 10.1017/pma.2023.2.

[45] C. M. Yakacki, R. Shandas, C. Lanning, B. Rech, A. Eckstein, and K. Gall, “Unconstrained recovery characterization of shape-memory polymer networks for cardiovascular applications,” *Biomaterials*, vol. 28, no. 14, pp. 2255–2263, May 2007, doi: 10.1016/j.biomaterials.2007.01.030.

[46] A. Lendlein and S. Kelch, “Shape-Memory Polymers,” *Angew. Chem. Int. Ed.*, vol. 41, no. 12, pp. 2034–2057, 2002, doi: 10.1002/1521-3773(20020617)41:12%3C2034::AID-ANIE2034%3E3.0.CO;2-M.

[47] H. Ramaraju, R. E. Akman, D. L. Safranski, and S. J. Hollister, “Designing Biodegradable Shape Memory Polymers for Tissue Repair,” *Adv. Funct. Mater.*, vol. 30, no. 44, p. 2002014, 2020, doi: 10.1002/adfm.202002014.

[48] S. S. Venkatraman, L. P. Tan, J. F. D. Joso, Y. C. F. Boey, and X. Wang, “Biodegradable stents with elastic memory,” *Biomaterials*, vol. 27, no. 8, pp. 1573–1578, Mar. 2006, doi: 10.1016/j.biomaterials.2005.09.002.

[49] R.-A. Y. Karina *et al.*, “Thermo-Shrinkable Biodegradable Polymers,” in *Biodegradable Polymers*, CRC Press, 2023.

[50] R. Duarah, Y. P. Singh, P. Gupta, B. B. Mandal, and N. Karak, “Smart self-tightening surgical suture from a tough bio-based hyperbranched polyurethane/reduced carbon dot nanocomposite,” *Biomed. Mater.*, vol. 13, no. 4, p. 045004, Apr. 2018, doi: 10.1088/1748-605X/aab93c.

[51] S. H. Choi and T. G. and Park, “Synthesis and characterization of elastic PLGA/PCL/PLGA tri-block copolymers,” *J. Biomater. Sci. Polym. Ed.*, vol. 13, no. 10, pp. 1163–1173, Jan. 2002, doi: 10.1163/156856202320813864.

[52] K. J. Cha, E. Lih, J. Choi, Y. K. Joung, D. J. Ahn, and D. K. Han, “Shape-Memory Effect by Specific Biodegradable Polymer Blending for Biomedical Applications,” *Macromol. Biosci.*, vol. 14, no. 5, pp. 667–678, 2014, doi: 10.1002/mabi.201300481.

[53] T. Nardo, Chiono ,Valeria, Gentile ,Piergiorgio, Tabrizian ,Maryam, and G. and Ciardelli, “Poly(DL-lactide-co-ε-caprolactone) and poly(DL-lactide-co-glycolide) blends for biomedical application: Physical properties, cell compatibility, and in vitro degradation behavior,” *Int. J. Polym. Mater. Polym. Biomater.*, vol. 65, no. 14, pp. 741–750, Sep. 2016, doi: 10.1080/00914037.2016.1163566.

[54] N. P. Tipnis and D. J. Burgess, “Sterilization of implantable polymer-based medical devices: A review,” *Int. J. Pharm.*, vol. 544, no. 2, pp. 455–460, Jun. 2018, doi: 10.1016/j.ijpharm.2017.12.003.

[55] C. K. Herczeg and J. Song, “Sterilization of Polymeric Implants: Challenges and Opportunities,” *ACS Appl. Bio Mater.*, vol. 5, no. 11, pp. 5077–5088, Nov. 2022, doi: 10.1021/acsabm.2c00793.

[56] J. Horakova *et al.*, “The effect of ethylene oxide sterilization on electrospun vascular grafts made from biodegradable polyesters,” *Mater. Sci. Eng. C*, vol. 92, pp. 132–142, Nov. 2018, doi: 10.1016/j.msec.2018.06.041.

[57] S. J. Peniston and S. J. Choi, “Effect of sterilization on the physicochemical properties of molded poly(L-lactic acid),” *J. Biomed. Mater. Res. B Appl. Biomater.*, vol. 80B, no. 1, pp. 67–77, 2007, doi: 10.1002/jbm.b.30570.

[58] M. H. Lee *et al.*, “Effects of low temperature hydrogen peroxide gas on sterilization and cytocompatibility of porous poly(d,l-lactic-*co*-glycolic acid) scaffolds,” *Surf. Coat. Technol.*, vol. 202, no. 22, pp. 5762–5767, Aug. 2008, doi: 10.1016/j.surfcoat.2008.06.114.

[59] T. A. M. Valente, D. M. Silva, P. S. Gomes, M. H. Fernandes, J. D. Santos, and V. Sencadas, “Effect of Sterilization Methods on Electrospun Poly(lactic acid) (PLA) Fiber Alignment for Biomedical Applications,” *ACS Appl. Mater. Interfaces*, vol. 8, no. 5, pp. 3241–3249, Feb. 2016, doi: 10.1021/acsami.5b10869.

[60] “ISO 13781:2017,” ISO. Accessed: Jul. 22, 2025. [Online]. Available: https://www.iso.org/standard/64565.html

[61] A. Ekinci, A. Gleadall, A. A. Johnson, L. Li, and X. Han, "Mechanical and hydrolytic properties of thin polylactic acid films by fused filament fabrication," *J. Mech. Behav. Biomed. Mater.*, vol. 114, p. 104217, Feb. 2021, doi: 10.1016/j.jmbbm.2020.104217.

[62] C. Min, W. Cui, J. Bei, and S. Wang, "Biodegradable shape-memory polymer—polylactide-co-poly(glycolide-co-caprolactone) multiblock copolymer," *Polym. Adv. Technol.*, vol. 16, no. 8, pp. 608–615, 2005, doi: 10.1002/pat.624.

[63] G. Schliecker, C. Schmidt, S. Fuchs, R. Wombacher, and T. Kissel, "Hydrolytic degradation of poly(lactide-co-glycolide) films: effect of oligomers on degradation rate and crystallinity," *Int. J. Pharm.*, vol. 266, no. 1, pp. 39–49, Nov. 2003, doi: 10.1016/S0378-5173(03)00379-X.

[64] B. Basu, "Mechanical Properties of Biomaterials," in *Biomaterials for Musculoskeletal Regeneration: Concepts*, B. Basu, Ed., Singapore: Springer, 2017, pp. 175–222. doi: 10.1007/978-981-10-3059-8_6.

[65] A. Grivet-Brancot, M. Boffito, and G. Ciardelli, "Use of Polyesters in Fused Deposition Modeling for Biomedical Applications," *Macromol. Biosci.*, vol. 22, no. 10, p. 2200039, 2022, doi: 10.1002/mabi.202200039.

[66] S. Hyuk Im, C. Yong Kim, Y. Jung, Y. Jang, and S. Hyun Kim, "Biodegradable vascular stents with high tensile and compressive strength: a novel strategy for applying monofilaments via solid-state drawing and shaped-annealing processes," *Biomater. Sci.*, vol. 5, no. 3, pp. 422–431, 2017, doi: 10.1039/C7BM00011A.

[67] M.-C. Lin, C.-W. Lou, J.-Y. Lin, T. A. Lin, Y.-S. Chen, and J.-H. Lin, "Biodegradable Polyvinyl Alcohol Vascular Stents: Structural Model and Mechanical and Biological Property Evaluation," *Mater. Sci. Eng. C*, vol. 91, pp. 404–413, Oct. 2018, doi: 10.1016/j.msec.2018.05.030.

[68] K. Gorna and S. Gogolewski, "Molecular stability, mechanical properties, surface characteristics and sterility of biodegradable polyurethanes treated with low-temperature plasma," *Polym. Degrad. Stab.*, vol. 79, no. 3, pp. 475–485, Mar. 2003, doi: 10.1016/S0141-3910(02)00363-4.

[69] E. Vey *et al.*, "Degradation mechanism of poly(lactic-*co*-glycolic) acid block copolymer cast films in phosphate buffer solution," *Polym. Degrad. Stab.*, vol. 93, no. 10, pp. 1869–1876, Oct. 2008, doi: 10.1016/j.polymdegradstab.2008.07.018.

[70] S. Li, "Hydrolytic degradation characteristics of aliphatic polyesters derived from lactic and glycolic acids," *J. Biomed. Mater. Res.*, vol. 48, no. 3, pp. 342–353, 1999, doi: 10.1002/(SICI)1097-4636(1999)48:3%3C342::AID-JBM20%3E3.0.CO;2-7.

Appendices

Appendix 1 Masses of Gamma-sterilized Samples

*No data, sample was used for imaging.

Sample number #	Initial dry weight (mg)	Degraded wet weight (mg)	Degraded dry weight (mg)	Day of degradation
1	6.9	7.1	6.6	3
2	7.6	7.7	7.3	3
3	7.5	7.7	7.2	3
4	6.1	7.6	6.0	7
5	9.8	11.4	9.7	7
6	5.7	6.9	5.7	7
7	8.0	12.2	7.3	10
8	8.6	12.2	7.6	10
9	8.6	12.0	7.4	10
10	8.3	*	*	*
11	7.8	*	*	*
12	11.5	*	*	*
13	7.0	6.9	6.1	14
14	7.4	6.4	5.7	14
15	7.3	7.5	5.8	14
16	7.0	3.8	3.3	17
17	6.1	3.2	2.7	17
18	6.8	4.3	3.4	17
19	7.4	2.4	2.1	21
20	7.5	2.1	1.8	21